Real-time Low-power VLSI Microsystem for Smart Acoustic Interfaces

Milutin Stanaćević

Stony Brook University

www.ece.stonybrook.edu/~milutin

milutin.stanacevic@stonybrook.edu

Outline

- **Motivation**
  - Audio interfaces
  - Directional hearing
- **Gradient Flow**
  - Principle: analysis of acoustic field using miniature arrays
  - Independent Component Analysis and Separation
- **Mixed-Signal VLSI Implementation**
  - Acoustic Localizer
  - ICA implementation for Multiple Source Separation
  - Reverberant Environment:
    - *Cochlear Filter Bank*
    - *Low Form-Factor ICA implementation*
- **Conclusion**

Motivation

- **"Cocktail Party" Problem**
  - The problem of source separation is intrinsically linked to the problem of source localization.
  - Resolving time and amplitude differences between observed sound waves is essential for effective localization and separation.

- **Human Auditory System**
  - The human auditory system performs remarkably well in segregating multiple streams of acoustic sources.
  - In relatively large animals where the distance between the ears is substantial relative to the wavelength of sound, interaural time, and intensity differences are large enough to be detectable by the central nervous system.

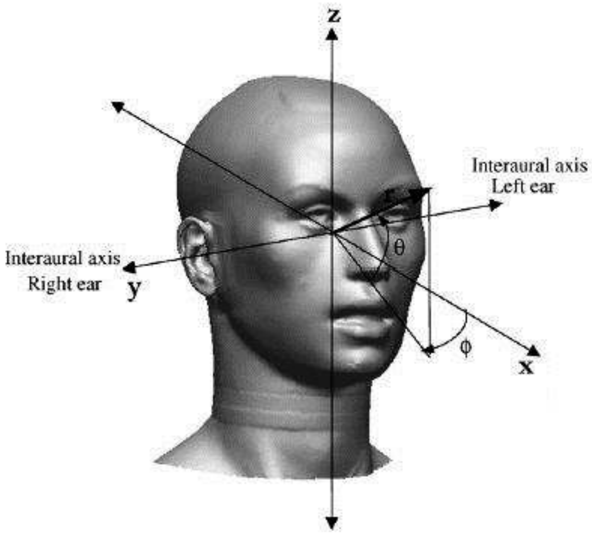

Audio Interfaces

- **Far-field noise cancellation for multimedia applications**
  - Siri, Google Now, Cortana

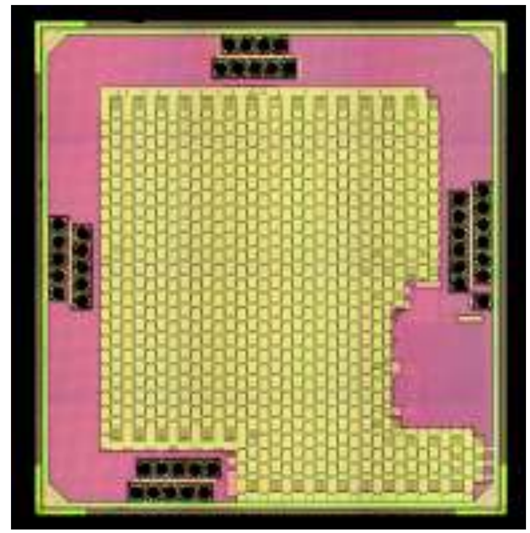

- **Audience's earSmart Technology**
  - Noise suppression with support for far-field
  - Siri made possible
- **Now in 8 of every 10 smartphones**
- **Hearing aids**

Motivation

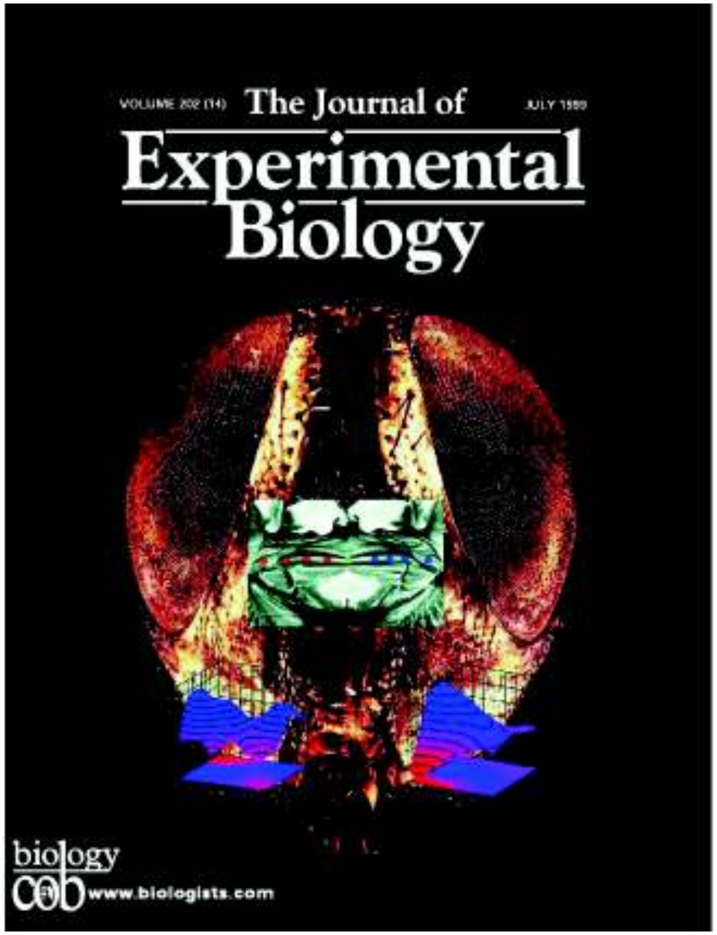

Robert, D., Miles, R.N. and Hoy, R.R., "Tympanal hearing in the sarcophagid parasitoid fly *Emblemasoma sp.*: the biomechanics of directional hearing," *J. Experimental Biology*, v. 202, pp. 1865-1876, 1999.

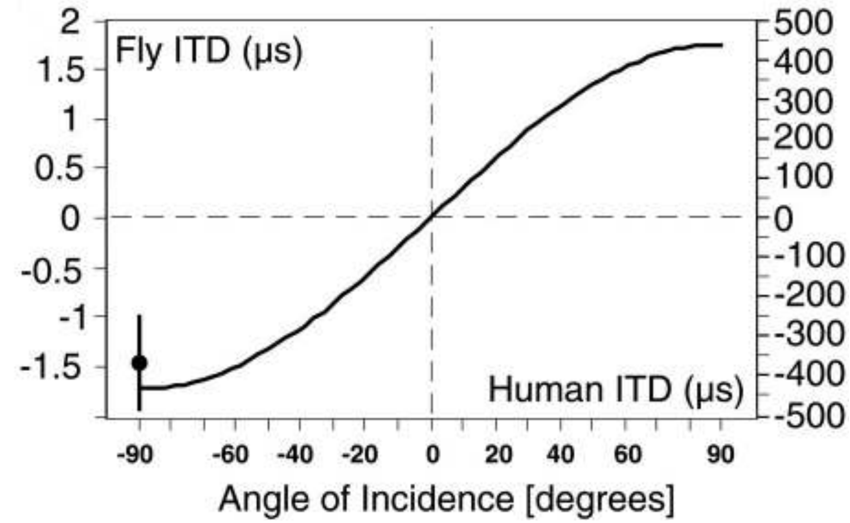

- **Directional hearing at sub-wavelength scale**
  - Parasitoid fly localizes sound-emitting target (cricket) by a beamforming acoustic sensor of dimensions a factor 100 smaller than the wavelength. 0.6mm ear separation comparing to 170mm of human ears
  - Tympanal beamforming organ senses acoustic pressure gradient, rather than time delays, in the incoming wave.

Hearing Aid Directionality

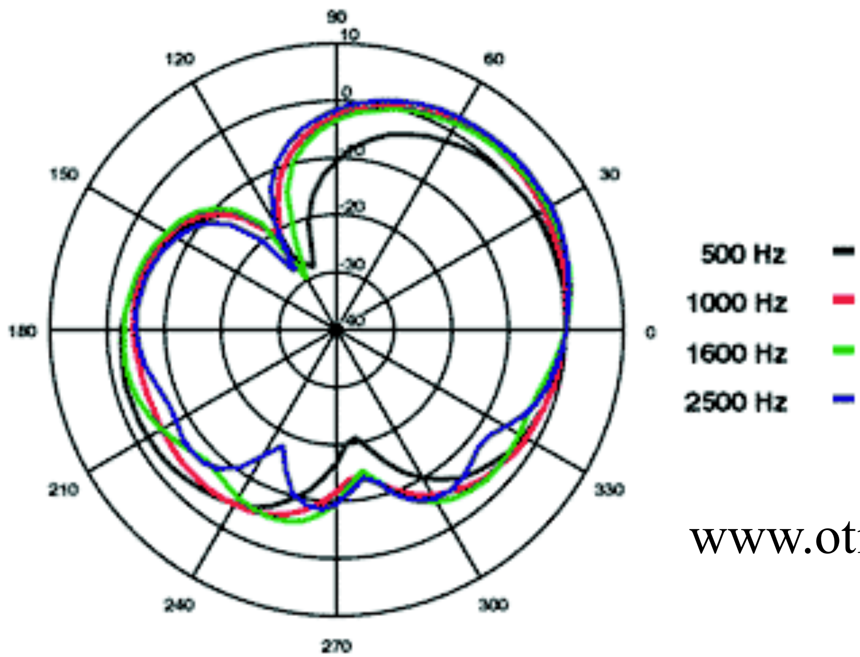

www.oticon.com

- Two microphones allow for one null angle in directionality pattern
- Adaptive beamforming allows to steer the null to noise source
- Presence of multiple noise sources requires source localization and separation with multiple microphones

Traveling Wave Source Localization

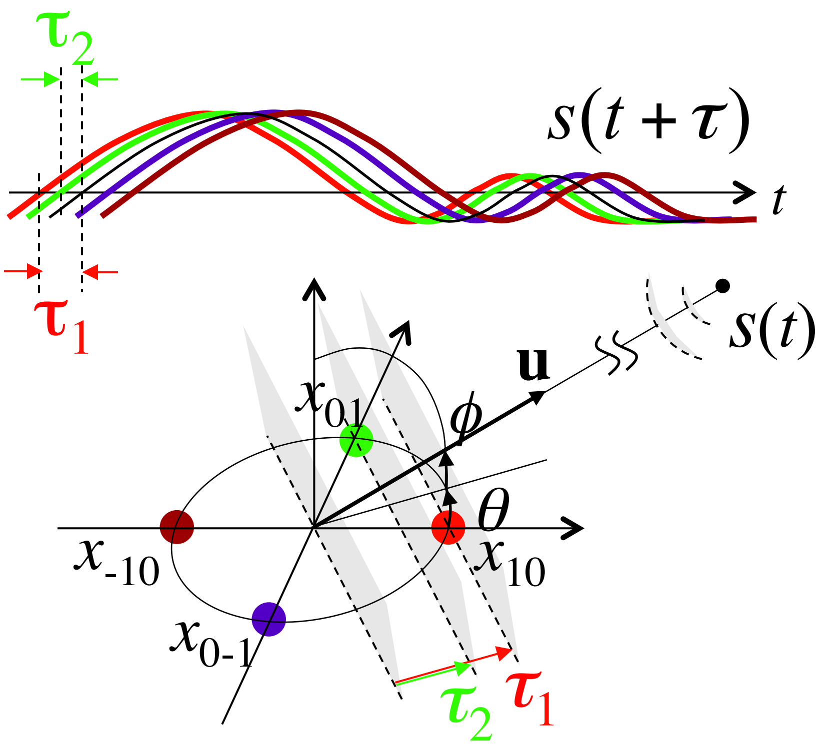

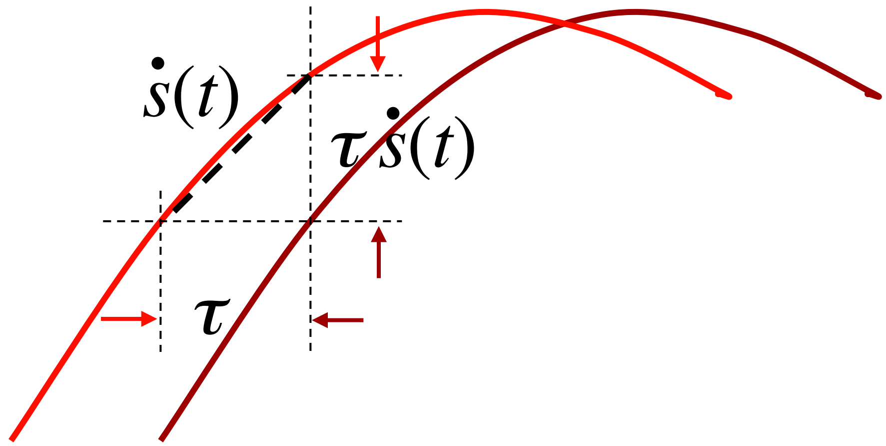

- Resolving time delays in wave propagation across array of low aperture requires sampling in excess of signal bandwidth, increasing power dissipation and noise bandwidth.

Gradient Flow Localization

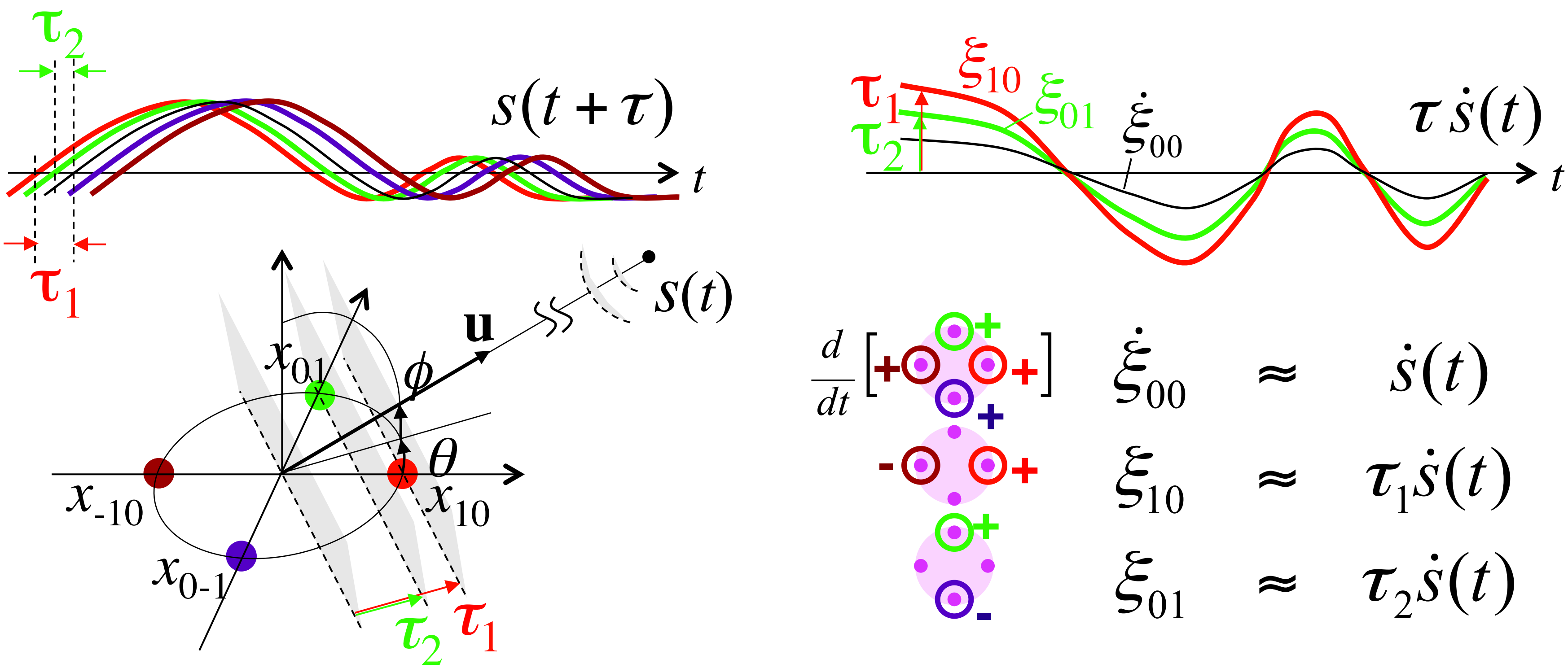

- Resolving time delays in wave propagation across array of low aperture requires sampling in excess of signal bandwidth, increasing power dissipation and noise bandwidth.
- *Gradient flow* obtains time delays at sub-sampling resolution by relating spatial and temporal differentials of the field across the array.

Gradient Flow Localization and Separation

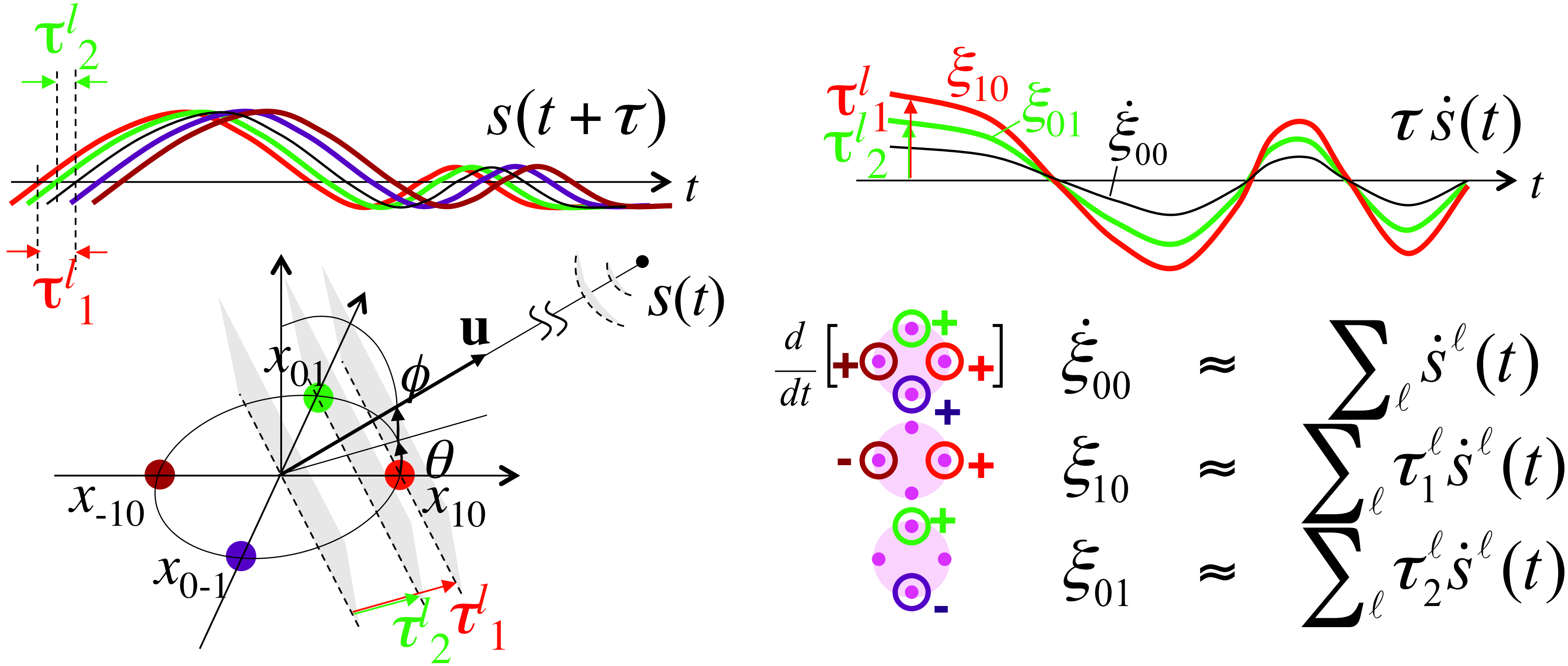

- Resolving time delays in wave propagation across array of low aperture requires sampling in excess of signal bandwidth, increasing power dissipation and noise bandwidth.
- *Gradient flow* obtains time delays at sub-sampling resolution by relating spatial and temporal differentials of the field across the array.

Separation and Localization

G. Cauwenberghs, M. Stanaćević and G. Zweig, U.S. Patent 6,865,490

Source mixtures are observed with additive sensor noise:

$$x_{pq}(t) = \sum_{\ell=1}^{L} s^{\ell}(t + \tau_{pq}^{\ell}) + n_{pq}(t)$$

Gradient flow reduces to a static (noisy) mixture problem:

$$\begin{bmatrix} \dot{\xi}_{00} \\ \xi_{10} \\ \xi_{01} \end{bmatrix} = \begin{bmatrix} 1 & \cdots & 1 \\ \tau_1^1 & \cdots & \tau_1^L \\ \tau_2^1 & \cdots & \tau_2^L \end{bmatrix} \begin{bmatrix} \dot{s}^1(t) \\ \vdots \\ \dot{s}^L(t) \end{bmatrix} + \begin{bmatrix} \dot{\nu}_{00} \\ \nu_{10} \\ \nu_{01} \end{bmatrix}$$

$$\mathbf{x} = \mathbf{A} \quad \mathbf{s} + \mathbf{n}$$

$\mathbf{x}$	$\mathbf{A}$	$\mathbf{s}$	$\mathbf{n}$
observations (gradients)	*direction vectors*	*sources* (time-differentiated)	*noise* (gradients)
	UNKNOWN	**UNKNOWN**	

Stony Brook University

Integrated Microsystems Lab

CAS 2016

Independent Component Analysis

- Blind source separation: separate and recover *independent* sources from mixed sensor observations.
- The sources and the mixing medium are assumed unknown.

Mixing model

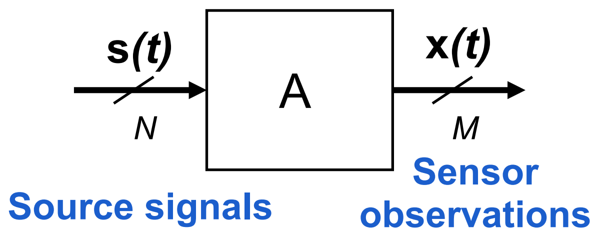

$$\mathbf{x} = \mathbf{A}\mathbf{s}$$

if A is a constant matrix:
linear static ICA problem

Solution (unmixing)

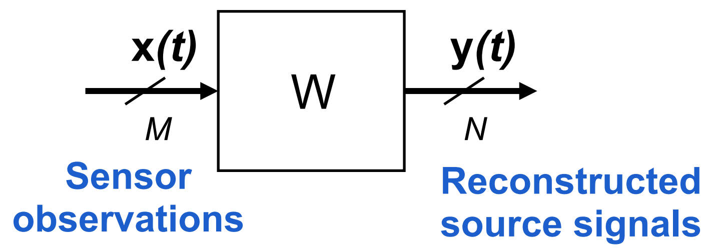

$$\mathbf{y} = \mathbf{W}\mathbf{x} \qquad (\mathbf{W}+\mathbf{I})\,\mathbf{y} = \mathbf{x}$$

Feedforward   Feedback

Independent Component Analysis

- **Independent component analysis (ICA) adaptively minimizes higher-order statistical dependencies between reconstructed signals to blindly estimate the unmixing matrix.**

	Unmixing model:	**Update rule:**
Jutten-Herault (1991)	$(\mathbf{W}+\mathbf{I})\,\mathbf{y} = \mathbf{x}$	$\Delta\mathbf{W} = \mu\ f(\mathbf{y})g(\mathbf{y}^T)$
InfoMax (*Bell and Sejnowski*, 1995)	$\mathbf{y} = \mathbf{W}\,\mathbf{x}$	$\Delta\mathbf{W} = \mu([\mathbf{W}^T]^{-1} - f(\mathbf{y})\mathbf{x}^T)$
Natural gradient (*Amari* 1996, …)	$\mathbf{y} = \mathbf{W}\,\mathbf{x}$	$\Delta\mathbf{W} = \mu(\mathbf{I} - f(\mathbf{y})\mathbf{y}^T)\mathbf{W}$

and many extensions…

Differential Sensitivity

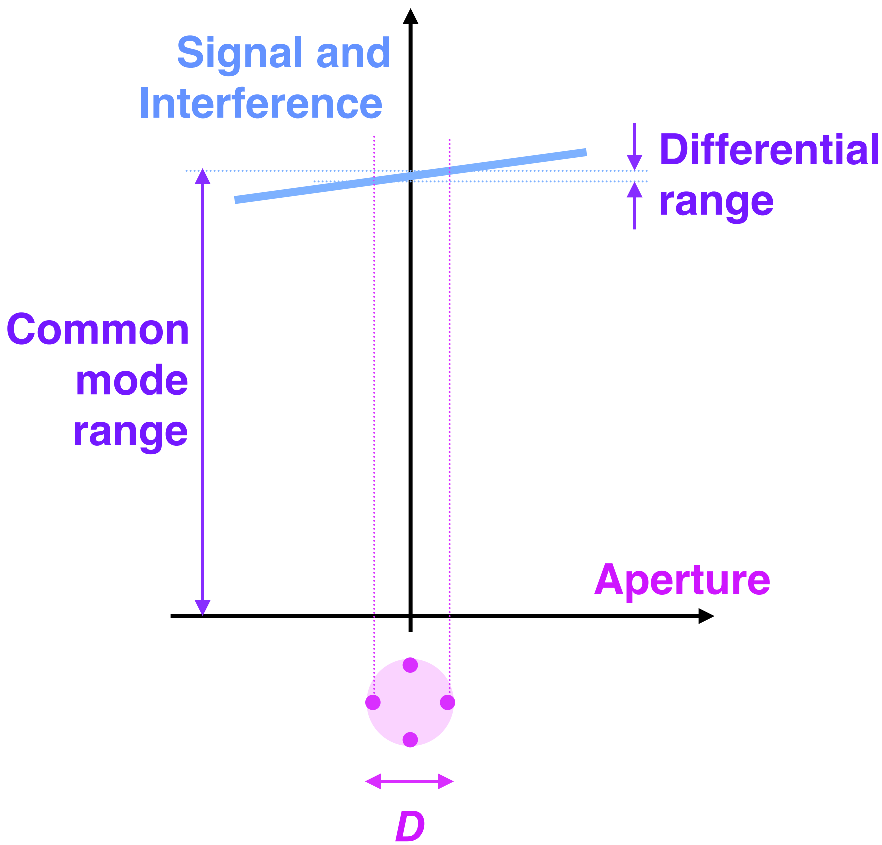

- **Gradient flow bearing resolution is fundamentally *independent* of aperture**
  - Assumes interference noise dominates sensor/ acquisition noise
- **In practice, aperture is limited by differential sensitivity in gradient acquisition**
  - Enhanced through differential coupling and common-mode suppression

Aperture Selection

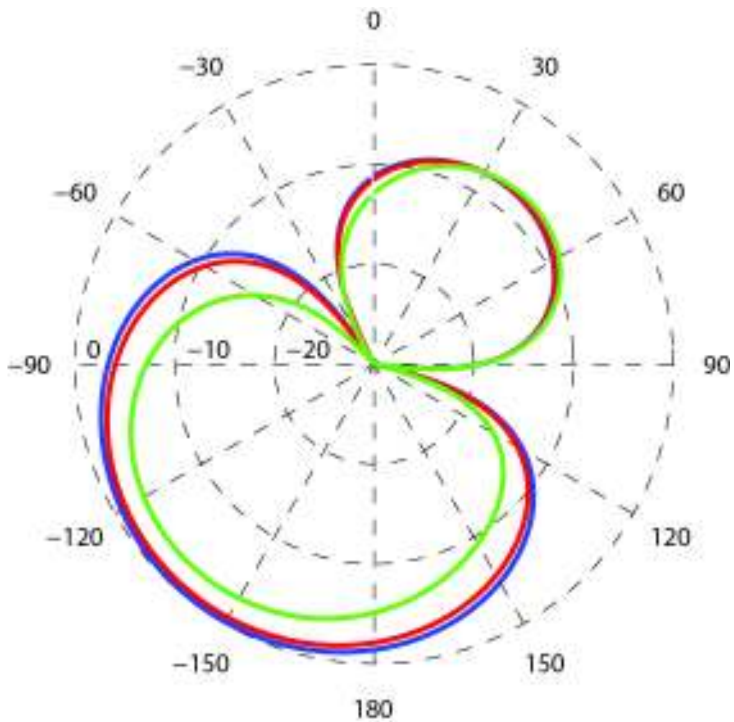

The beampattern for the impinging 8 kHz acoustic source as a function of the unit grid size (0.5cm, 1cm, 2cm) of the microphone array. The canceled interfering directional source signals originate from azimuth angles of θ_2=-30^o and θ_3=100^o.

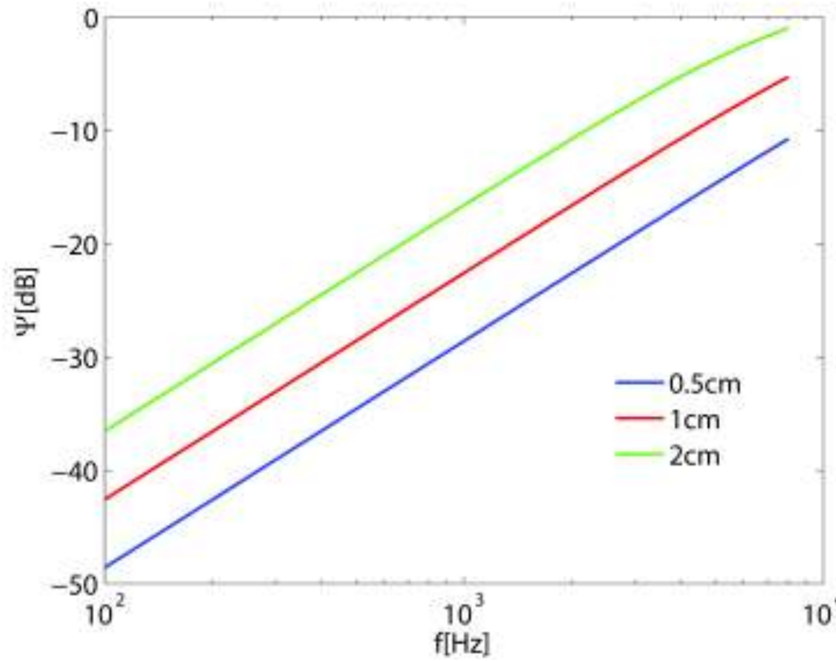

The noise sensitivity, the transfer function of the signal-to-noise ratio from the observed signals to the integrated reconstructed sources, shown for three different apertures of the microphone array, 0.5cm, 1cm and 2cm.

Separation Performance

S. Li and M. Stanaćević, " Analysis of Gradient Flow Technique for Blind Source Localization and Separation using Miniature Microphone Arrays“ TASSP (in review)

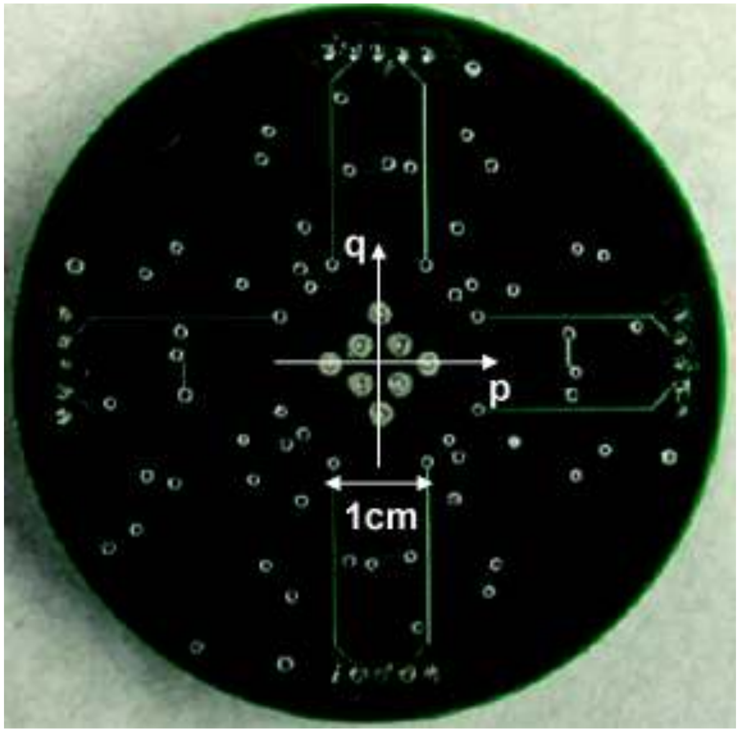

Photo of the printed circuit board with the microphone array and signal conditioning circuitry.

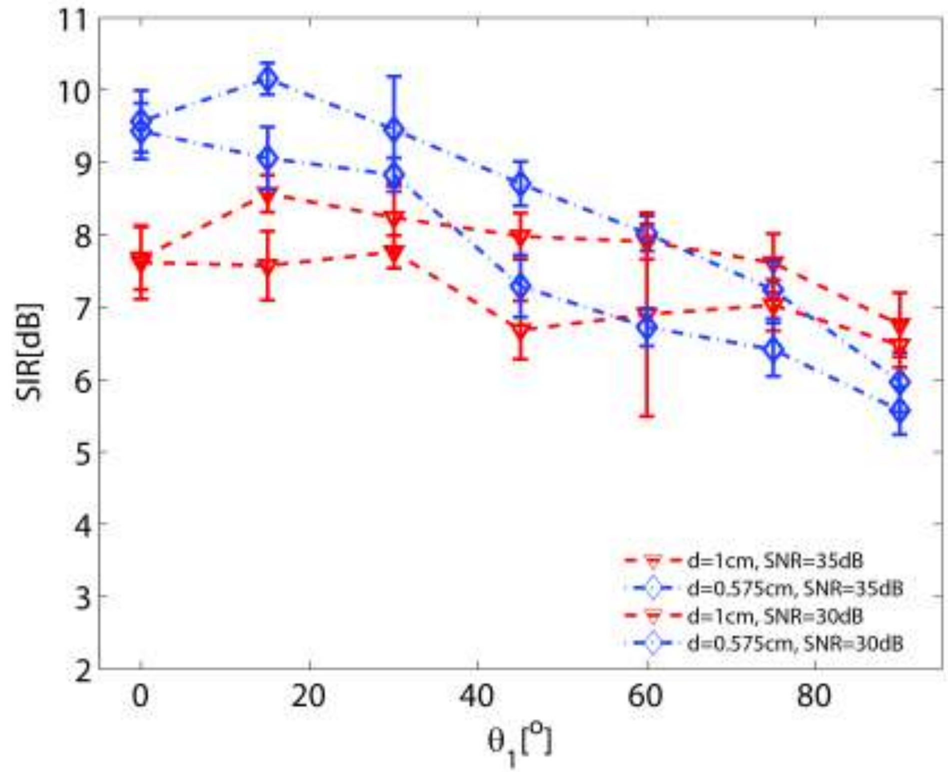

The separation of the first speech source signal from the two directional interfering speech signals as a function of incidence angle θ_1 for two different signal-to-noise ratios at the microphones. The incidence angles of the second and third source are $\theta_2 = 150^o$ and $\theta_3 = 165^o$.

Mixed-Signal VLSI Implementation: Single Source Localization

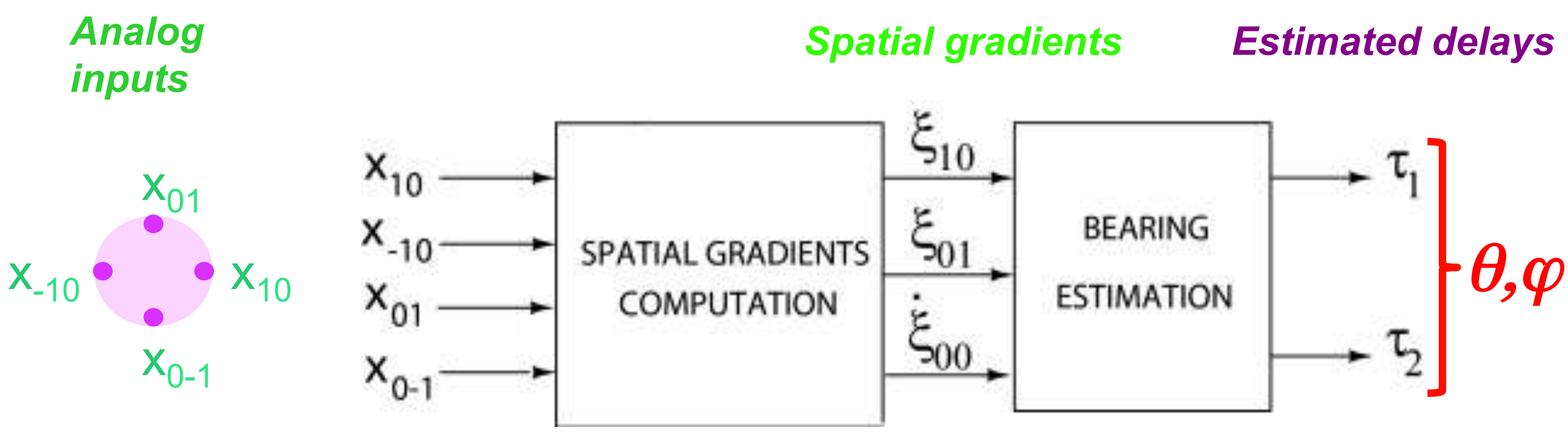

$$\xi_{10} \approx \tau_1 \dot{\xi}_{00}$$

$$\xi_{01} \approx \tau_2 \dot{\xi}_{00}$$

Mixed-Signal VLSI Implementation: Multiple Source Separation and Localization

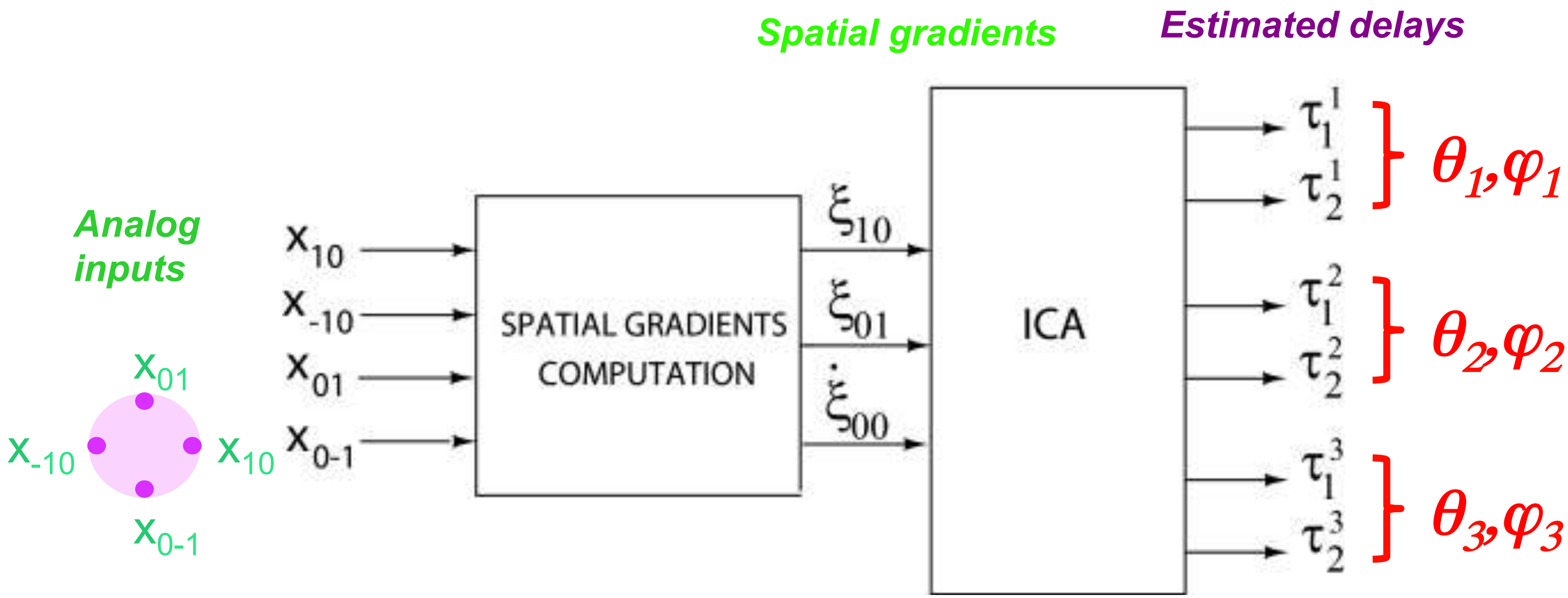

$$\begin{bmatrix}\dot{\xi}_{00}\\ \xi_{10}\\ \xi_{01}\end{bmatrix} = \begin{bmatrix}1 & 1 & 1\\ \tau_1^1 & \tau_1^2 & \tau_1^3\\ \tau_2^1 & \tau_2^2 & \tau_2^3\end{bmatrix}\begin{bmatrix}\dot{s}^1(t)\\ \dot{s}^2(t)\\ \dot{s}^3(t)\end{bmatrix} + \begin{bmatrix}\dot{\nu}_{00}\\ \nu_{10}\\ \nu_{01}\end{bmatrix}$$

Spatial Gradient Computation

Analog inputs

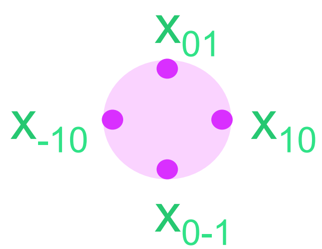

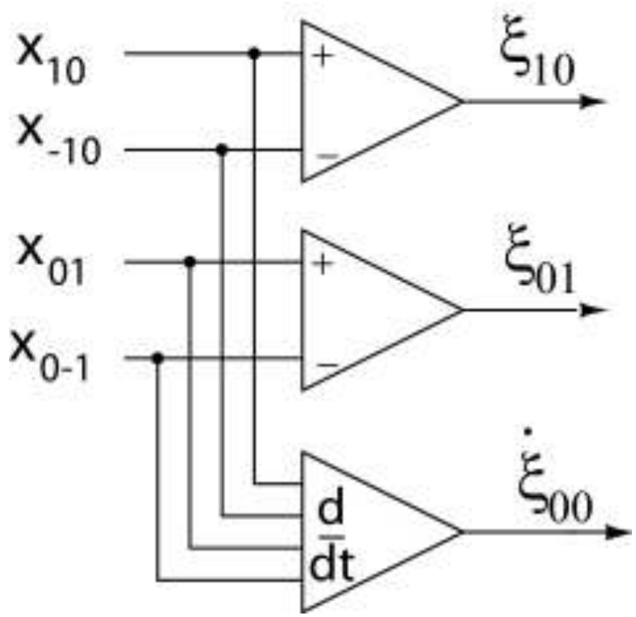

Temporal derivative of average and estimated first-order spatial gradients

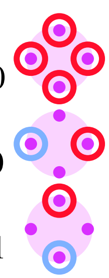

$$\xi_{00} \quad \frac{1}{4}(x_{-1,0} + x_{1,0} + x_{0,-1} + x_{0,1})$$

$$\xi_{10} \quad \frac{1}{2}(x_{1,0} - x_{-1,0})$$

$$\xi_{01} \quad \frac{1}{2}(x_{0,1} - x_{0,-1})$$

CDS Differential Sensing

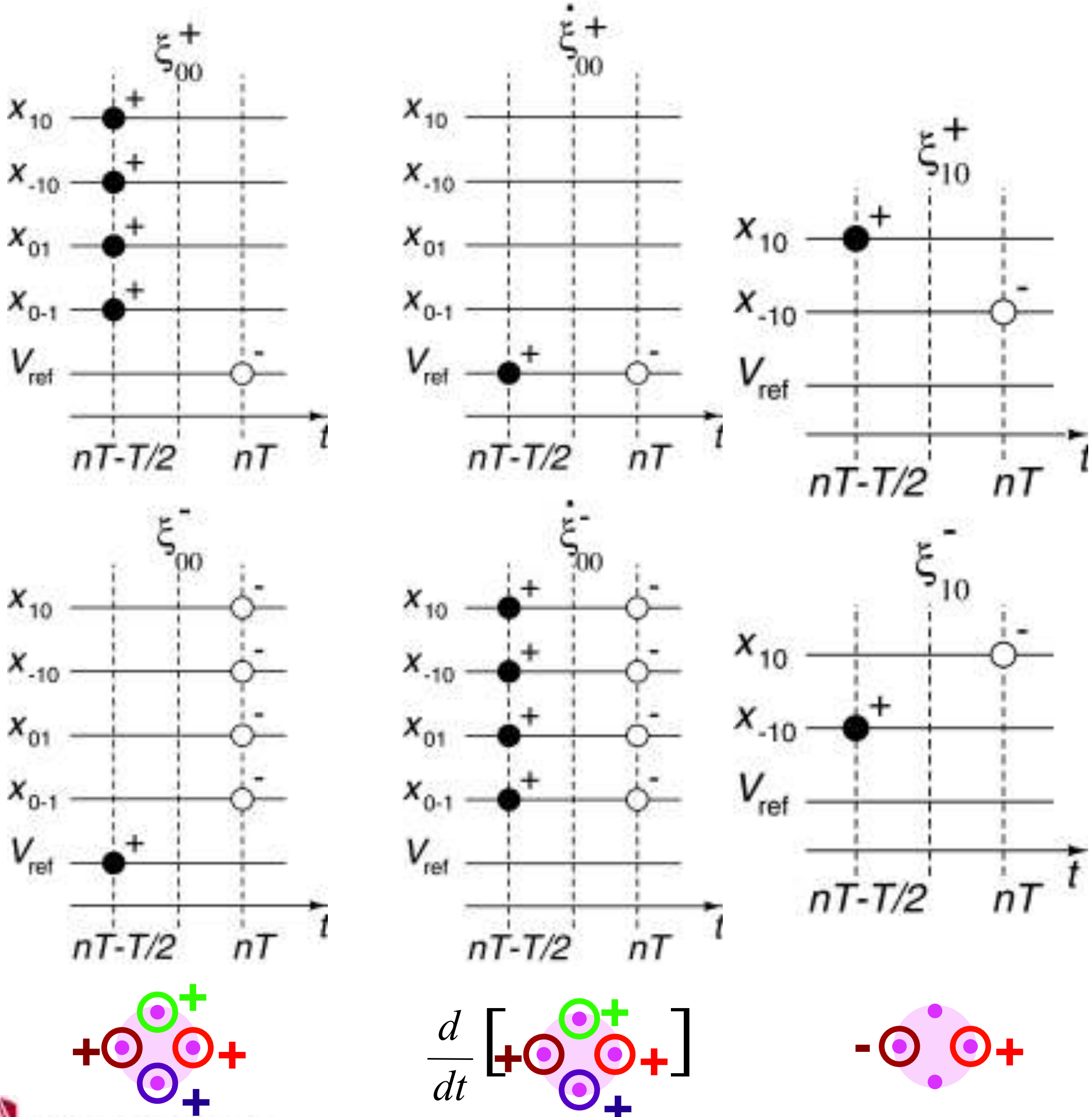

Switched-capacitor, discrete-time analog signal processing

– Correlated Double Sampling (CDS)
  - *Offset cancellation and 1/f noise reduction*

– Fully differential
  - *Clock and supply feedthrough rejection*

First-order spatial gradient computation

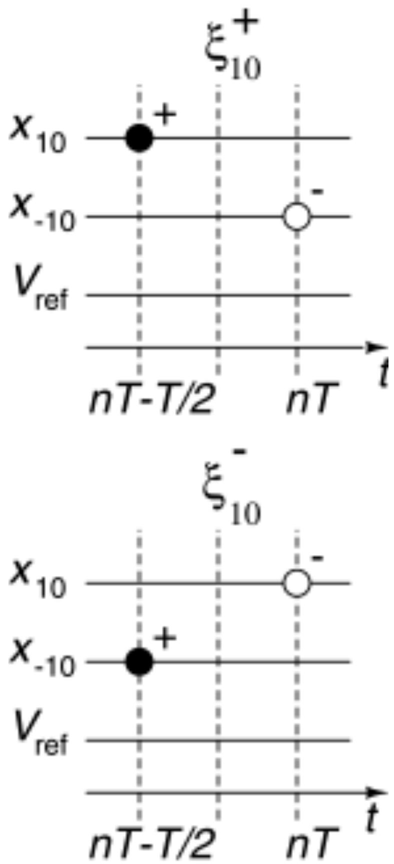

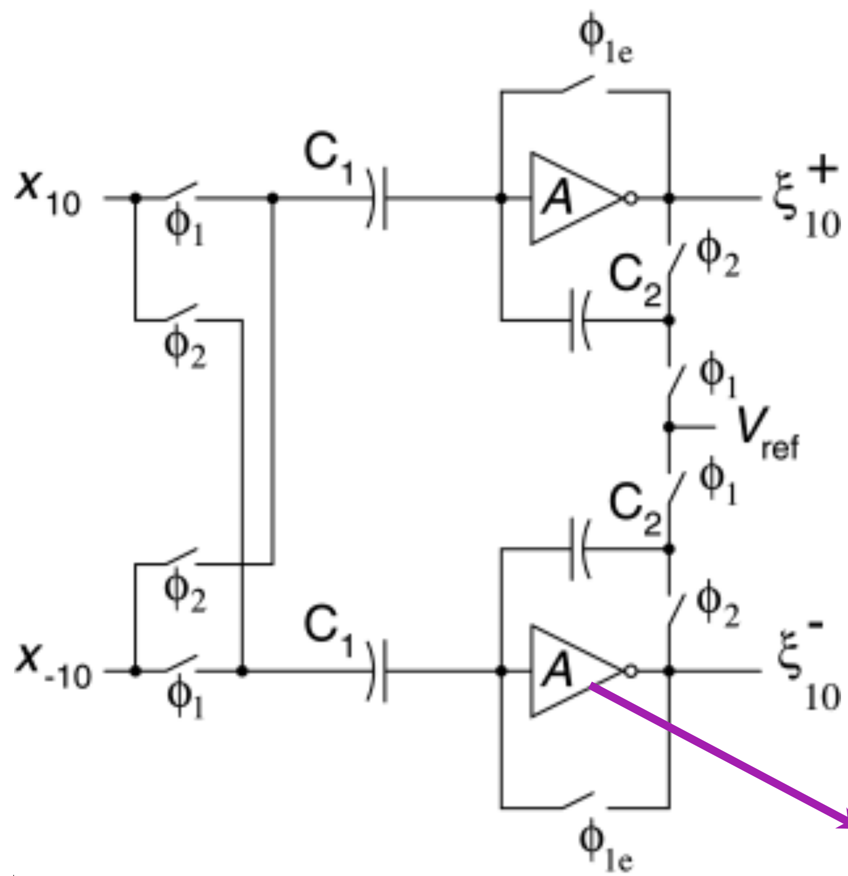

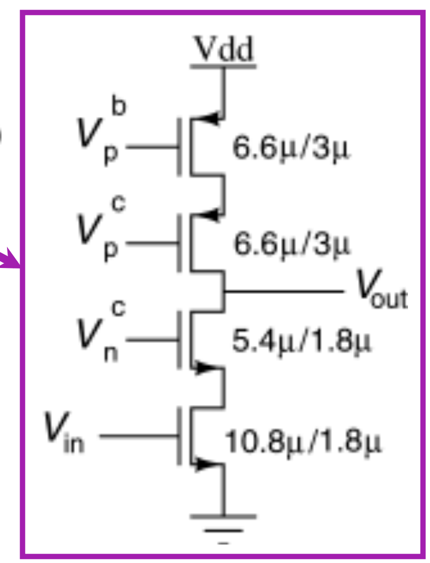

$$\hat{\xi}^{+}_{10}[n] = x_{10}[n-\frac{1}{2}] - x_{-10}[n]$$

$$\hat{\xi}^{-}_{10}[n] = x_{-10}[n-\frac{1}{2}] - x_{10}[n]$$

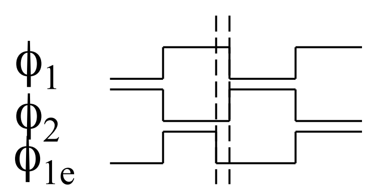

Adaptive Common-Mode Suppression

Systematic common-mode error in finite-difference gradients:

due to gain mismatch across sensors in the array:

$\hat{\xi}_{00}$ 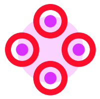 $$\tfrac{1}{4}(x_{-1,0}+x_{1,0}+x_{0,-1}+x_{0,1}) \approx \xi_{00} \approx \sum_\ell s^\ell(t)$$

$\hat{\xi}_{10}$ 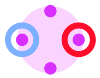 $$\tfrac{1}{2}(x_{1,0}-x_{-1,0}) \approx \xi_{10}+\varepsilon_1\xi_{00} \approx \sum_\ell \tau_1{}^\ell \dot{s}^\ell(t)+\varepsilon_1\sum_\ell s^\ell(t)$$

$\hat{\xi}_{01}$ 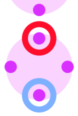 $$\tfrac{1}{2}(x_{0,1}-x_{0,-1}) \approx \xi_{01}+\varepsilon_2\xi_{00} \approx \sum_\ell \tau_2{}^\ell \dot{s}^\ell(t)+\varepsilon_2\sum_\ell s^\ell(t)$$

can be eliminated using second order statistics only:

$$\mathrm{E}[\dot{s}^\ell(t)s^m(t)]=0,\quad \forall \ell,m \quad \Rightarrow \quad \begin{cases}\mathrm{E}[\xi_{00}\xi_{10}]=0\\ \mathrm{E}[\xi_{00}\xi_{01}]=0\end{cases}$$

Adaptive LMS calibration:

$$\xi_{10} \approx \hat{\xi}_{10} - \frac{\mathrm{E}[\hat{\xi}_{00}\hat{\xi}_{10}]}{\mathrm{E}[\hat{\xi}_{00}{}^2]}\hat{\xi}_{00}$$

$$\xi_{01} \approx \hat{\xi}_{01} - \frac{\mathrm{E}[\hat{\xi}_{00}\hat{\xi}_{01}]}{\mathrm{E}[\hat{\xi}_{00}{}^2]}\hat{\xi}_{00}$$

Spatial Gradient Computation with Common-mode Suppression

Analog inputs

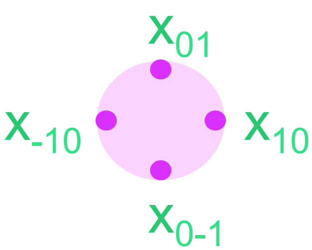

Average, temporal derivative and estimated spatial gradients

Spatial gradients with suppressed common-mode

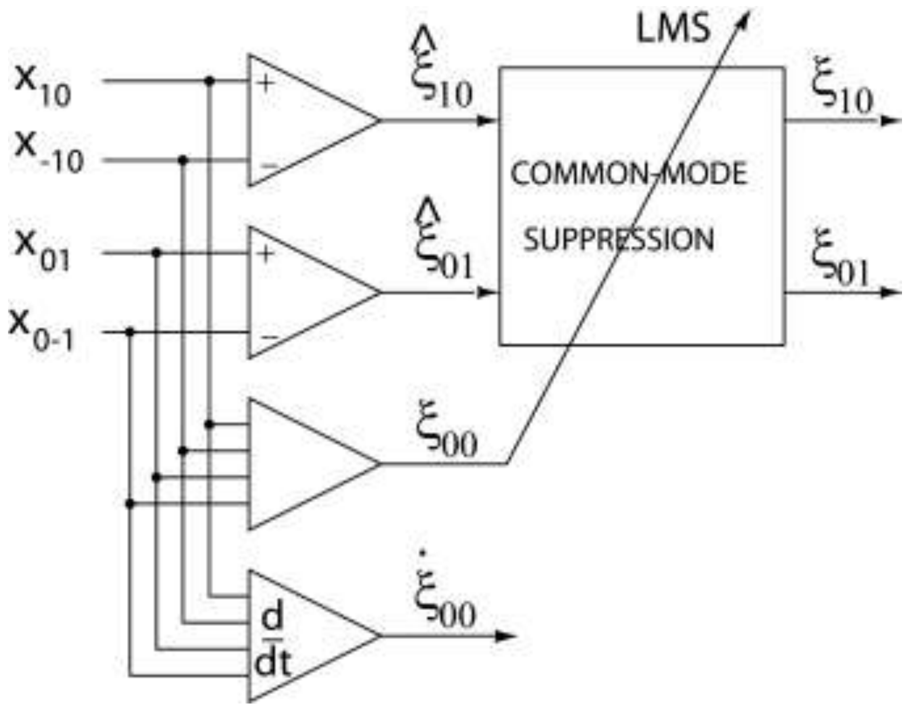

Source Localization: Mixed-Signal LMS Adaptation

$$\xi_{10} \approx \tau_1 \dot{\xi}_{00}$$

- **Sign-sign LMS differential on-line adaptation rule**
  - Delay parameter estimation :

$$e_{10}^{+}[n] = \xi_{10}^{+}[n] - (\tau_1^{+} \dot{\xi}_{00}^{+}[n] + \tau_1^{-} \dot{\xi}_{00}^{-}[n])$$

$$e_{10}^{-}[n] = \xi_{10}^{-}[n] - (\tau_1^{-} \dot{\xi}_{00}^{+}[n] + \tau_1^{+} \dot{\xi}_{00}^{-}[n])$$

$$\tau_1^{+}[n+1] = \tau_1^{+}[n] + \mathrm{sgn}(e_{10}^{+}[n] - e_{10}^{-}[n])\,\mathrm{sgn}(\dot{\xi}_{00}^{+}[n] - \dot{\xi}_{00}^{-}[n])$$

$$\tau_1^{-} = 2^{n} - 1 - \tau_1^{+}$$

- **Digital storage and update of parameter estimates**
  - 12-bit counter
  - 8-bit multiplying DAC to construct LMS error signal

Mixed-signal LMS Implementation

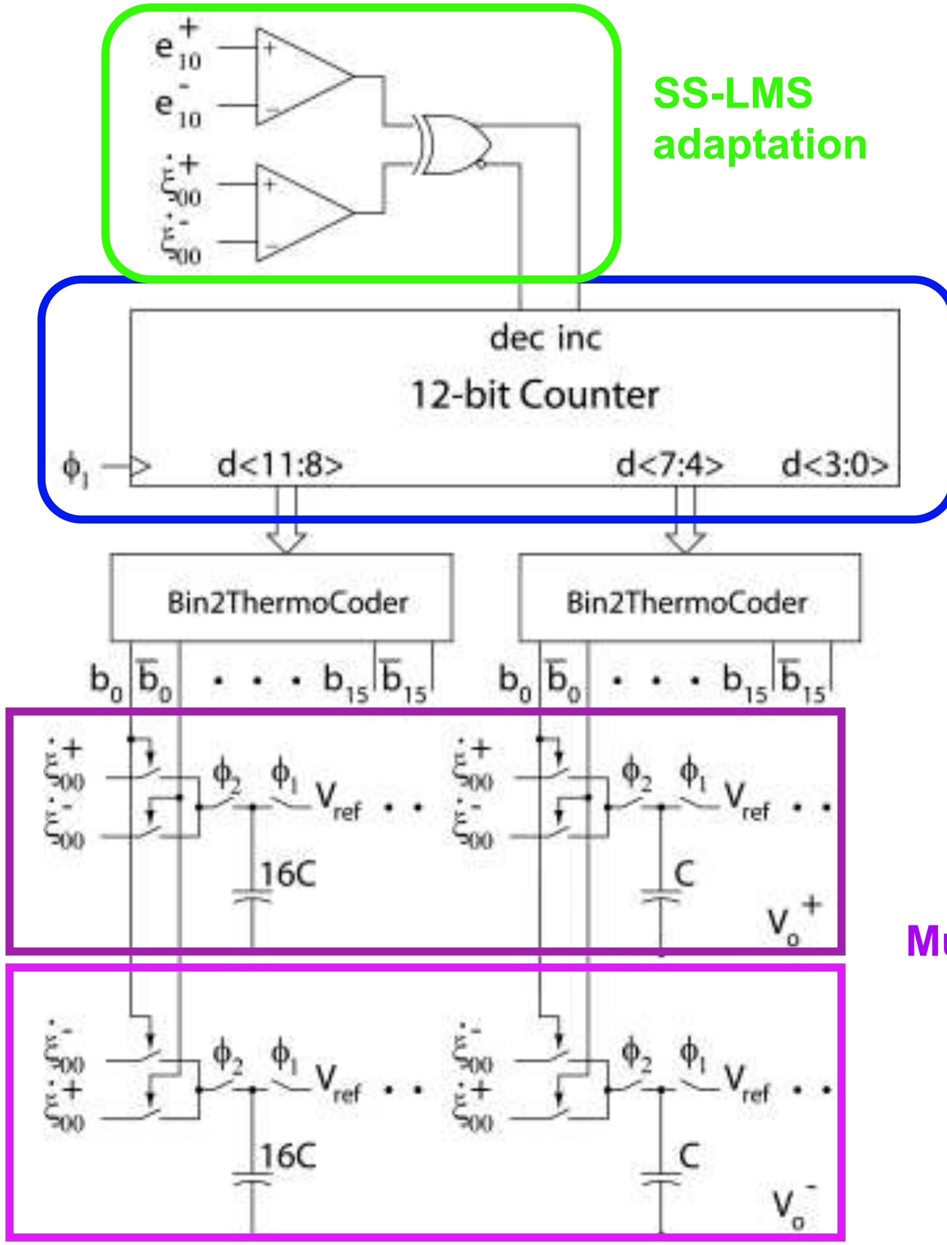

SS-LMS adaptation

12-bit estimated parameter

Multiplying DACs

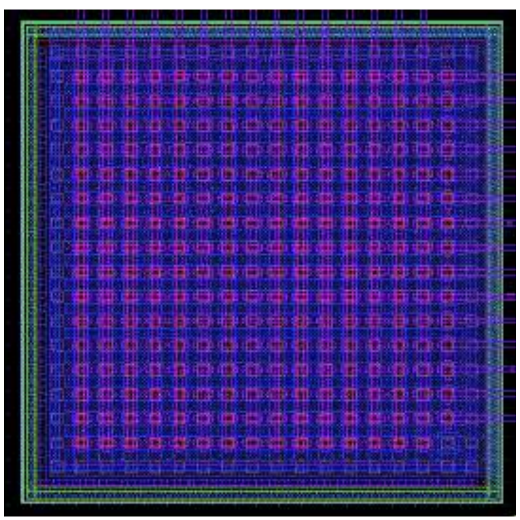

16 x 16 DAC array

Stony Brook University

Common-mode compensated spatial gradient

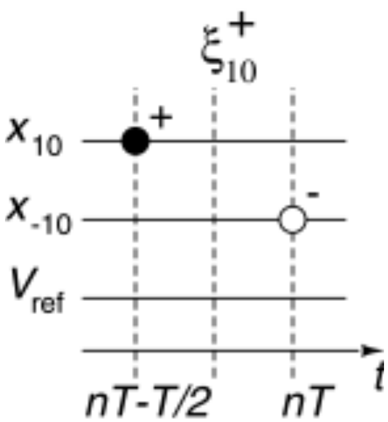

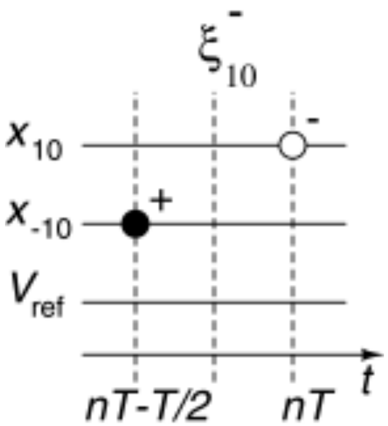

$$\hat{\xi}^{+}_{10}[n] = x_{10}[n-\frac{1}{2}] - x_{-10}[n]$$

$$\hat{\xi}^{-}_{10}[n] = x_{-10}[n-\frac{1}{2}] - x_{10}[n]$$

Multiplying DAC for common-mode compensation

Uncompensated first-order spatial gradient computation along p-direction

T-cell attenuates output swing

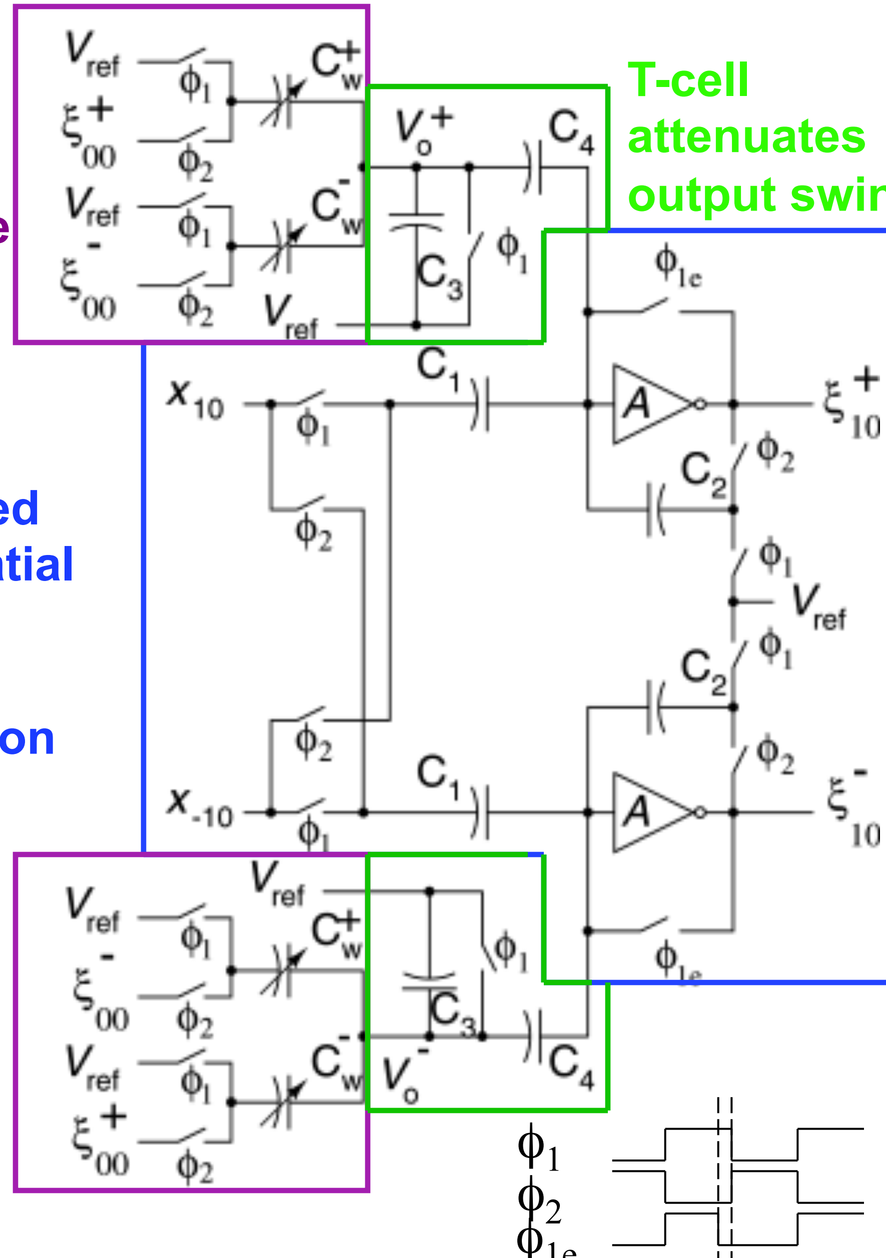

Gradient Flow Localizer

M. Stanaćević and G. Cauwenberghs, "Micropower Gradient Flow VLSI Acoustic Localizer“ TCAS 2005.

- Digital LMS adaptive 3-D bearing estimation
  - *Analog microphone inputs*
  - *Digital bearing outputs*
  - *Analog gradient outputs*
- 3*mm* x 3*mm* in 0.5μ*m* 3M2P CMOS
- 8-bit effective digital resolution
  - *2μs at 2 kHz*
  - *0.25μs at 16 kHz*
- Power dissipation
  - *32 μW at 2 kHz*
  - *54 μW at 16 kHz*

Localization Performance

- **One directional source in room environment: *Band-limited (100-1000Hz) Gaussian signal presented through loudspeaker***
  - **distance between microphones : 2.5 cm**
  - **distance between loudspeaker and sensor array : 1 m**
  - **sampling frequency 16 kHz**
  - **SNR around 35 dB**

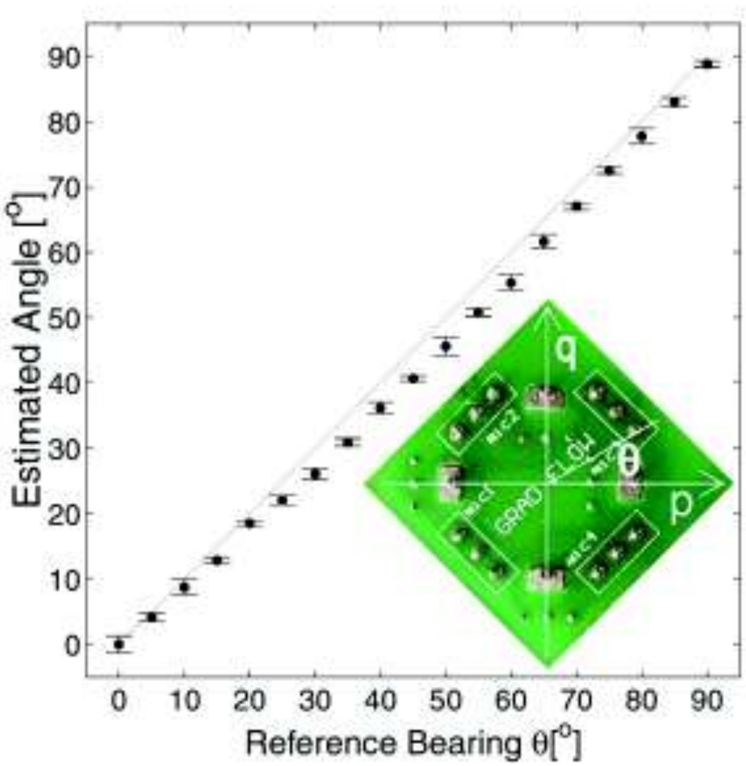

Source localization with 5 degree increments

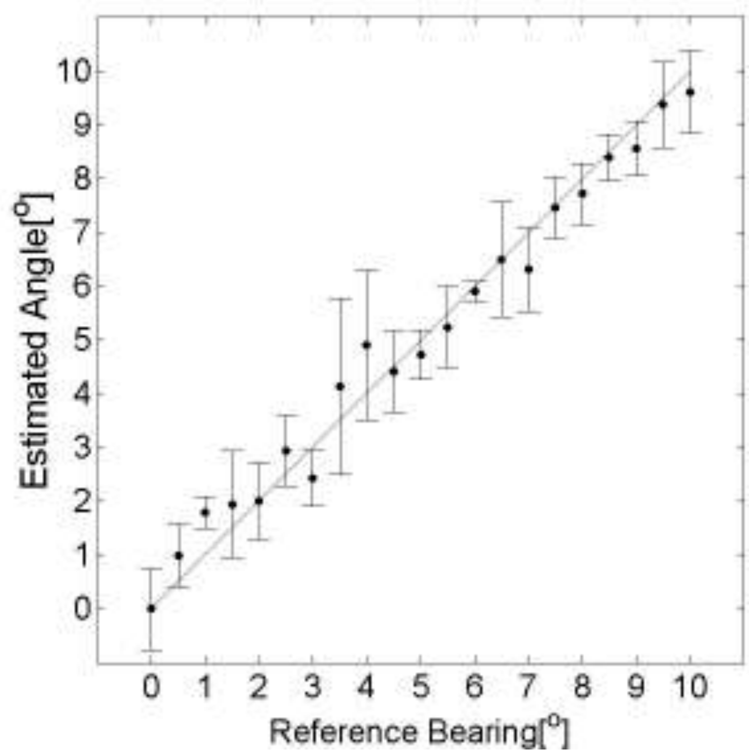

Source localization with 0.5 degree increments

Open-field Vehicle Tracking

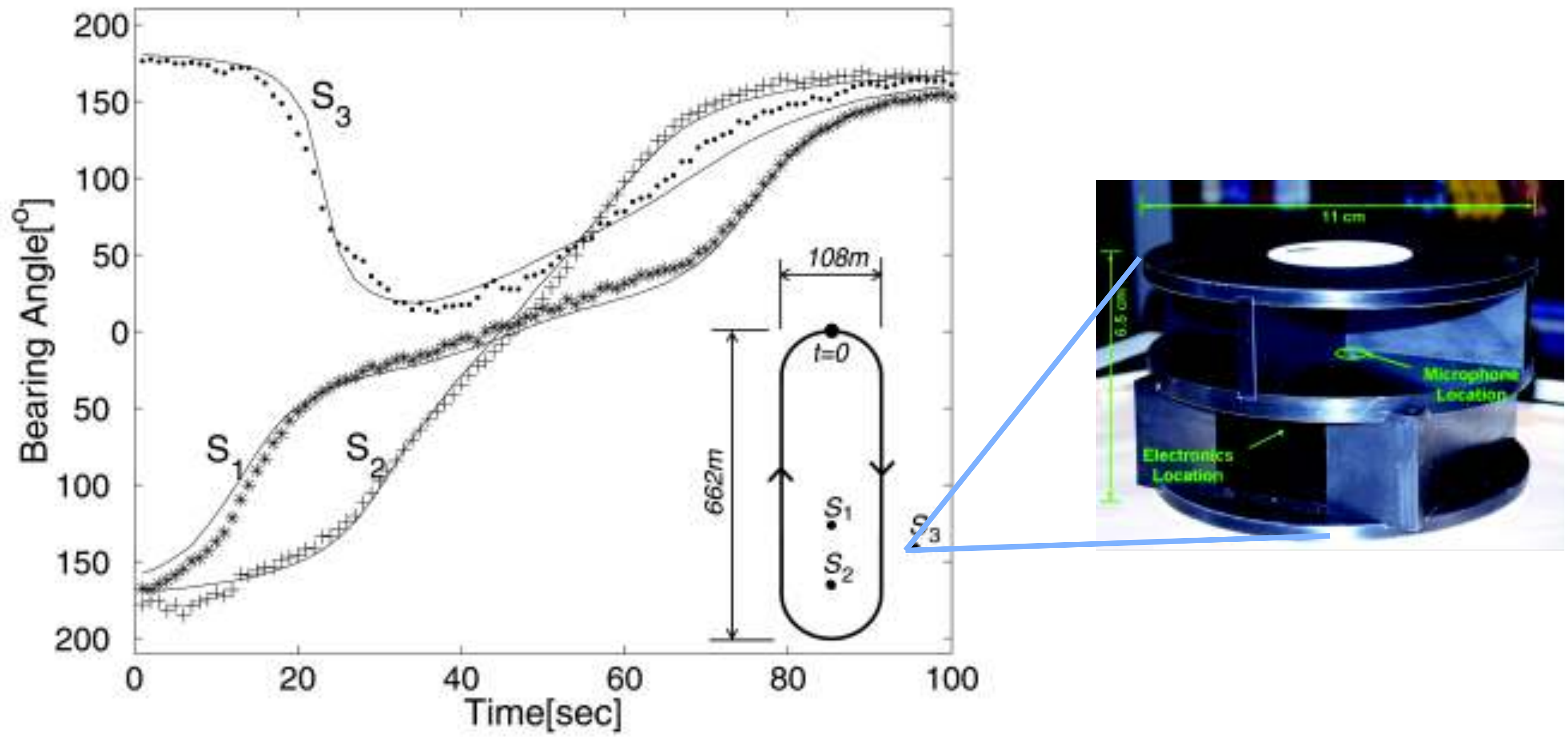

- **Acoustic Surveillance Unit (ASU) with integrated *GradFlow* ASIC**
- **Aberdeen Proving Grounds field tests**
  - Sensor network with 3 ASUs
  - 5 degree bearing accuracy in tracking ground vehicles over 600m range
  - Detection of overflying aircraft, tracking azimuth & elevation

ICA Implementation

- **HJ learning rule**

$$(\mathbf{W}+\mathbf{I})\,\mathbf{y}=\mathbf{x} \qquad \mathbf{y}=(\mathbf{W}+\mathbf{I})^{-1}\,\mathbf{x}\approx(\mathbf{I}-\mathbf{W})\mathbf{x}$$

vector-matrix multiplication

$$\Delta\mathbf{W}=\mu\; f(\mathbf{y})g(\mathbf{y}^T)$$

$$\Delta W=\begin{cases}-\mu f(y_i)g(y_j) & i\neq j\\ 0 & i=j\end{cases}$$

outer-product learning rule

- **NG learning rule**

$$\mathbf{y}=\mathbf{W}\mathbf{x}$$

vector-matrix multiplication

$$\Delta\mathbf{W}=\mu(\mathbf{I}-f(\mathbf{y})\mathbf{y}^T)\mathbf{W}=\mu\mathbf{W}-\mu f(\mathbf{y})\mathbf{z}^T \qquad \mathbf{z}=\mathbf{W}^T\mathbf{y}$$

vector-matrix multiplication

$$\Delta w_{ij}=\mu w_{ij}-\mu\, f(y_i)z_j$$

outer-product learning rule

ICA System Diagram

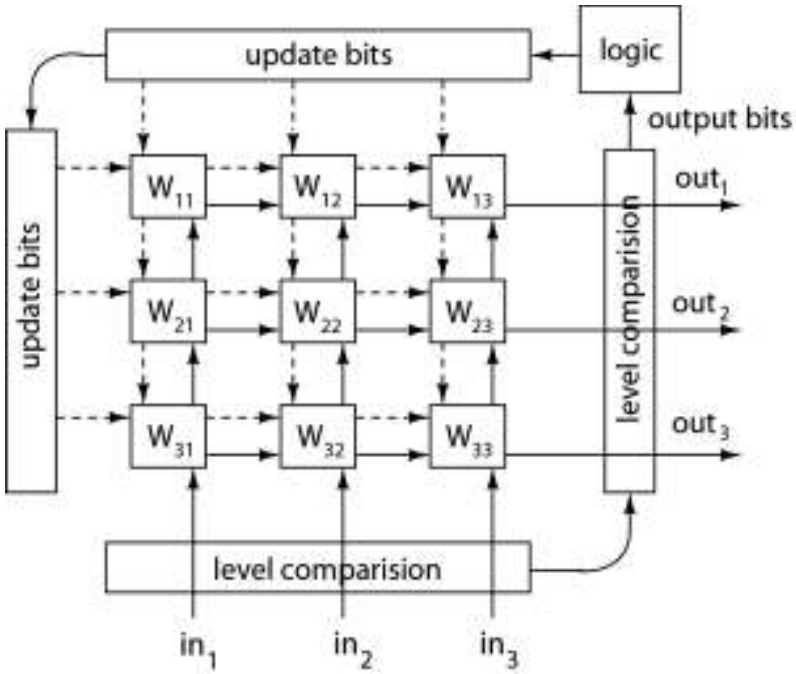

System block diagram

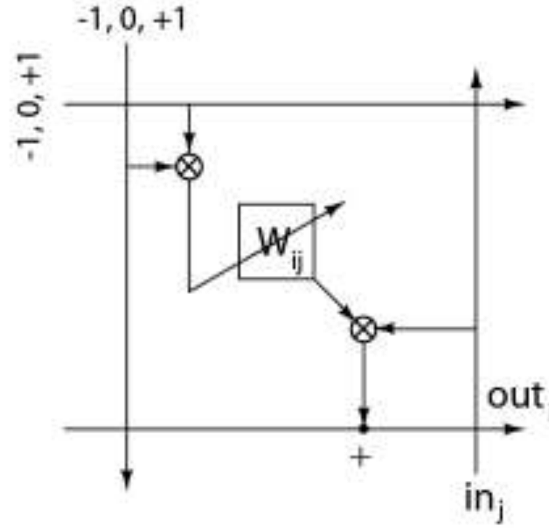

Cell functionality

- **Digitally reconfigurable ICA update rule**
  - $\Delta w_{ij} = \mu w_{ij} - \mu f(y_i) z_j$
  - $f(y_i) = \mathrm{sign}(y_i)$, and 3-level quantization of z_j

ICA SC implementation

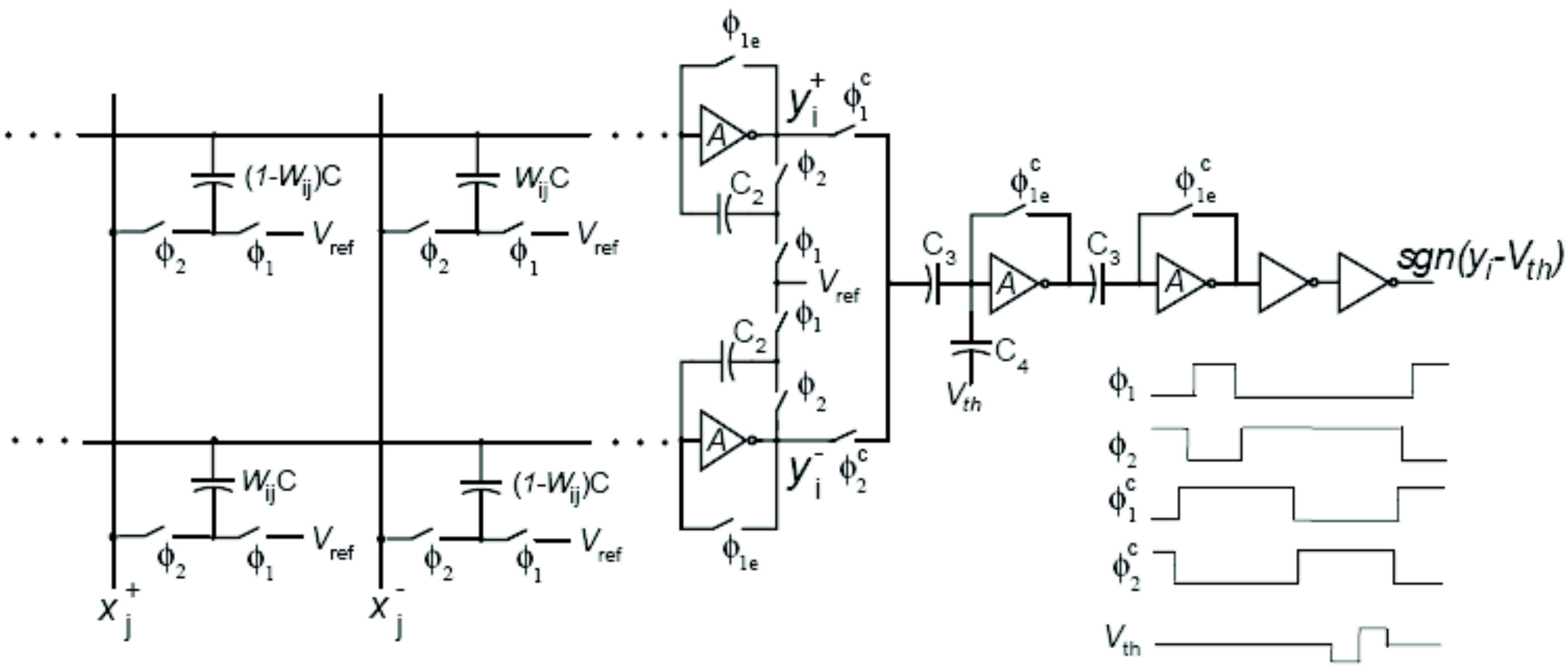

- **Digital storage and update of weight coefficients**
  - 14-bit counter
  - 8-bit multiplying DAC to construct output signal

ICA VLSI Processor

M. Stanaćević, S. Li and G. Cauwenberghs, "Micropower Mixed-signal VLSI Independent Component Analysis for Gradient Flow Acoustic Source Separation“ TCAS (in review)

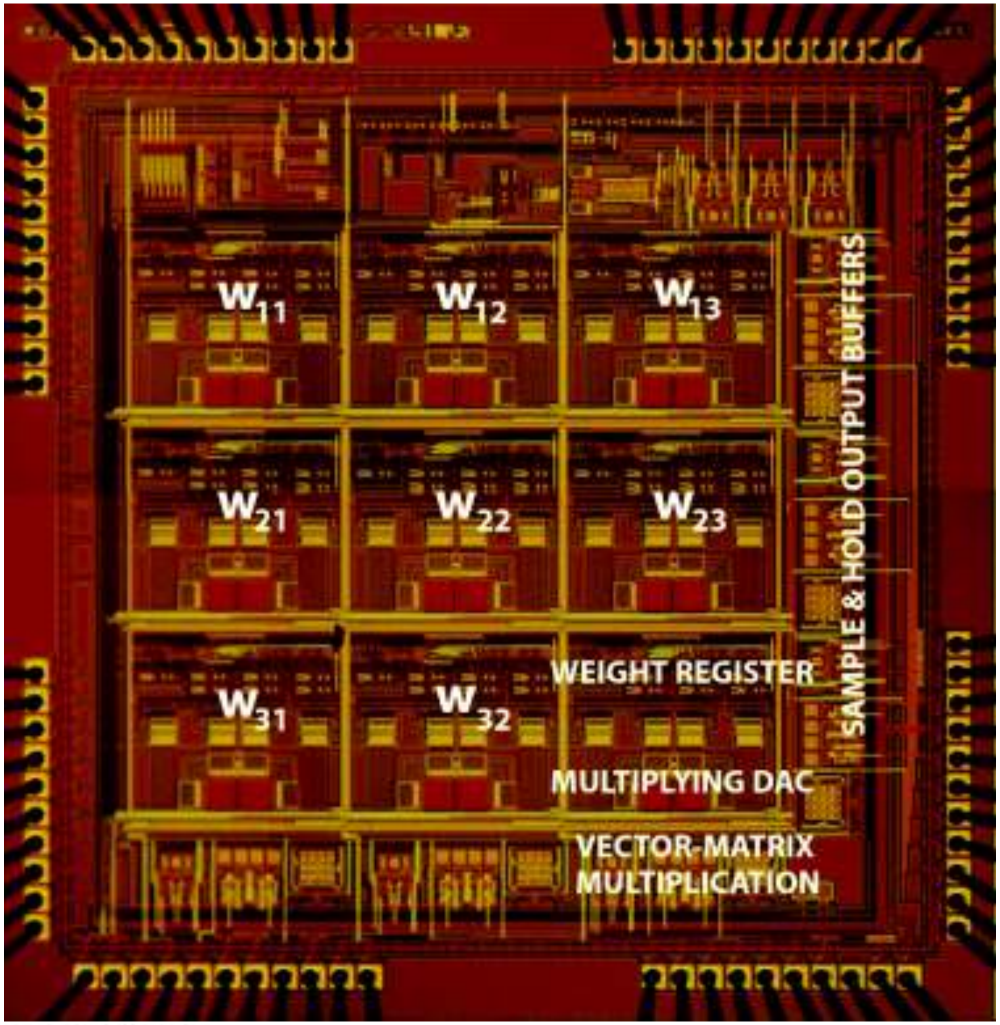

- 3 inputs – sensor signals or gradient flow signals
- 3 outputs – estimated sources
- 14-bit digital estimates of unmixing coefficients
- 3*mm* x 3*mm* in 0.5μ*m* CMOS
- 192μW power consumption at 16kHz

Gradient Flow Source Separation

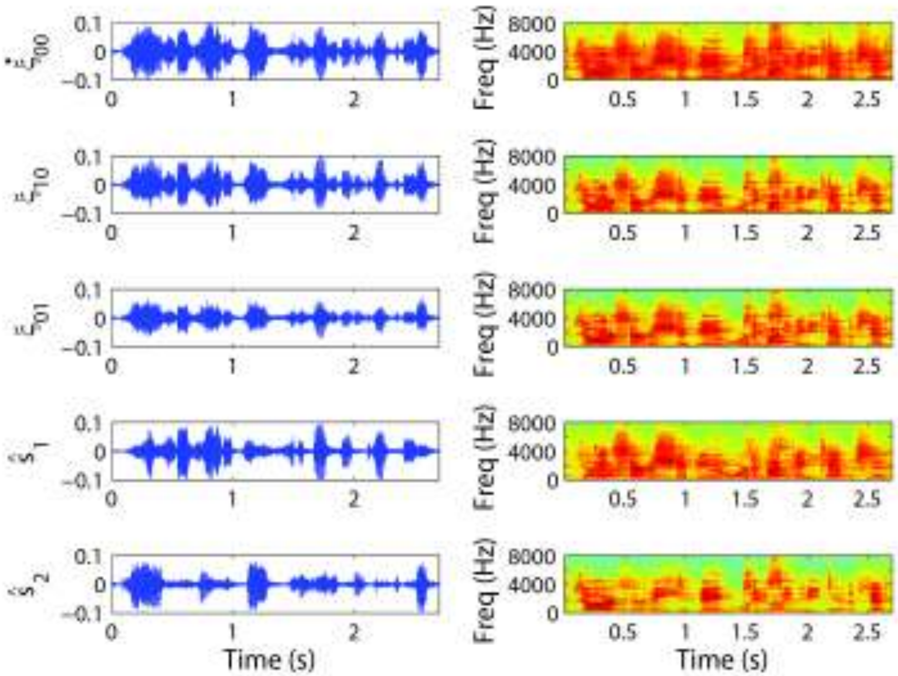

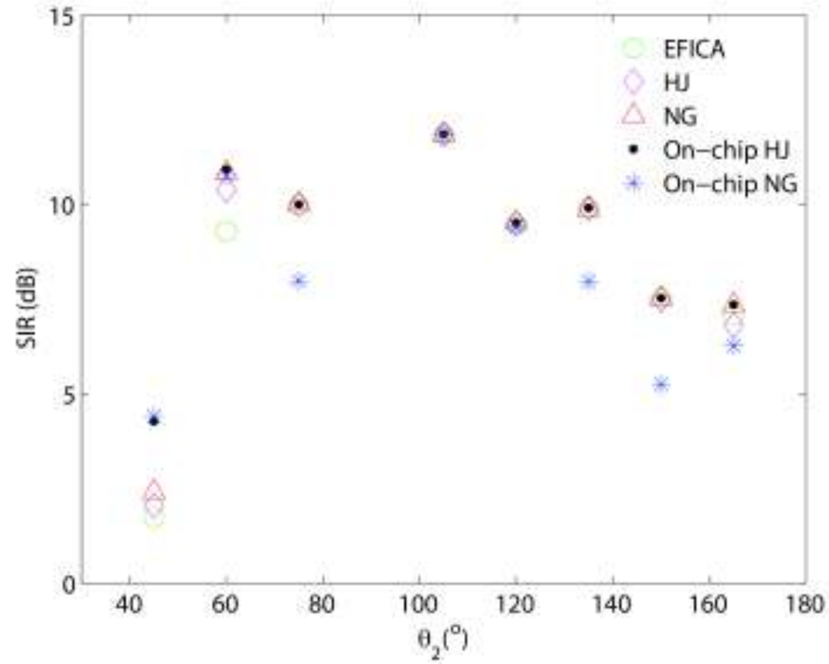

Time waveforms and spectrograms of spatial gradients, input signals to the ICA processor, and reconstructed source signals, output signals of the ICA processor for the case of two source signals with azimuth angles of $\theta_1 = 30^o$ and $\theta_2 = 105^o$.

SIR for two reconstructed speech sources played through a loudspeakers to a miniature microphone array in a conference room. The azimuth angle of the first source was fixed at $\theta_1 = 30^o$ and the azimuth angle of the second source θ_2 was varied from 45^o to 135^o. The elevation angles ϕ_1 and ϕ_2 for both sources were 8^o.

Separation in Reverberant Environment

- In a reverberant environment, the multi-path wave propagation contributes delayed mixture components to the observations.

$$x_i(t) = \sum_{j=1}^{N} h_{ij} * s_j(t)$$

- Frequency domain techniques are attractive for solving the convolutive mixtures, as the convolution becomes product in the frequency domain.

$$X_i(\omega) = \sum_{j=1}^{N} H_{ij}(\omega) S_j(\omega)$$

- The mixing matrix are dependent on the frequency, but can be considered constant in a narrow band.

- So we propose the subband ICA architecture that decomposes gradients into subbands and applies static ICA separately in each frequency band

Subband ICA Separation Architecture

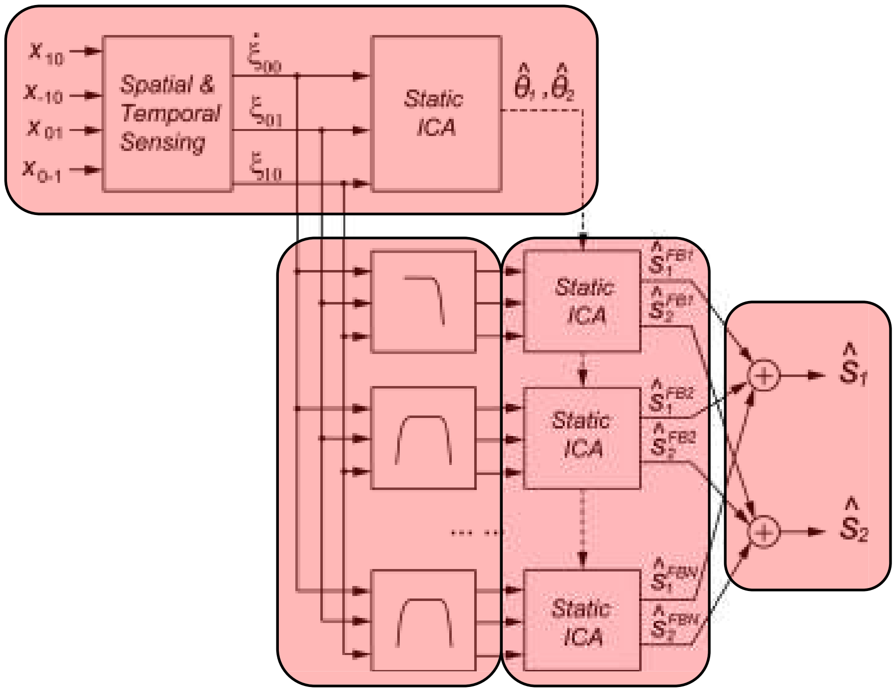

Block diagram of the proposed subband gradient flow ICA architecture.

1. Localization results from full-band static ICA are obtained as directional cues.

2. 16-channel filterbank is used to decompose the spatial gradient signals.

3. Static ICA algorithm is used in each frequency band to obtain the unmixing matrix and signal estimation.

4. Signals from each band is aligned and synthesized to reconstruct full-band estimations.

Subband ICA

- **Subband deposition with 16 filterbanks in mel scale (0-1kHz in linear scale, 1kHz-8kHz in log scale)**
- **Initial Condition**
  - Use fullband unmixing matrix as initial condition in each bin to ensure fast and robust convergence
- **Permutation Ambiguity**
  - Directional information in each band is compared with fullband localization to align estimations from the same source
  - If directional information strongly deviates from the fullband result in a certain band, then fullband unmixing matrix overwrites
- **Scaling Ambiguity**
  - Scaling resolver from the estimated mixing matrix is reapplied to ensure the uniformity of amplitude across all frequency bands

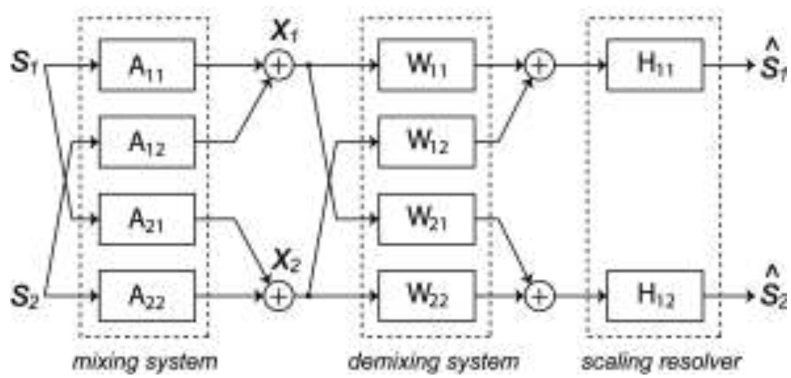

Subband Gradient Flow Source Separation

S. Li and M. Stanaćević, "Subband Gradient Flow Acoustic Source Separation for Moderate Reverberation Environment", Asilomar 2012.

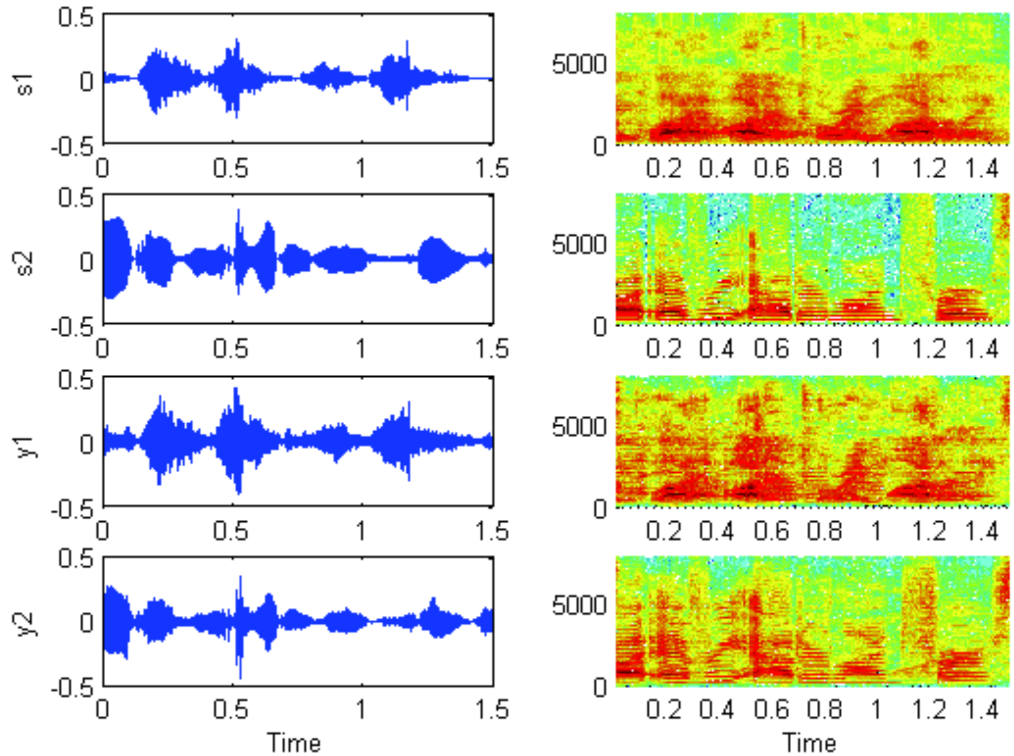

Comparison of Static ICA and Subband ICA Results				
	RT_{60} = 200ms		RT_{60} = 300ms	
	SIR1	SIR2	SIR1	SIR2
Static ICA	25.30dB	26.91dB	6.95dB	12.80dB
Subband ICA	24.65dB	28.99dB	10.12dB	15.75dB

Subband Decomposition: VLSI Implementation

- 16 channels from 150Hz to 10kHz (from 150Hz to 1kHz 8 channels in linear space and from 1kHz to 10kHz 8 channels in logarithmic space)
- High linearity and wide dynamic range are required due to the linear mixing model
- Small chip area
- Low power consumption

Band-pass Filter Structure

- Gm-C filter with capacitive attenuation, attenuation ratio: A_1=19, A_3=4
- Gain = 1, Q = 4, $|V_x| = |V_y|$
- Fully differential OTA, $G_{m1}=G_{m2}=4G_{m3}$

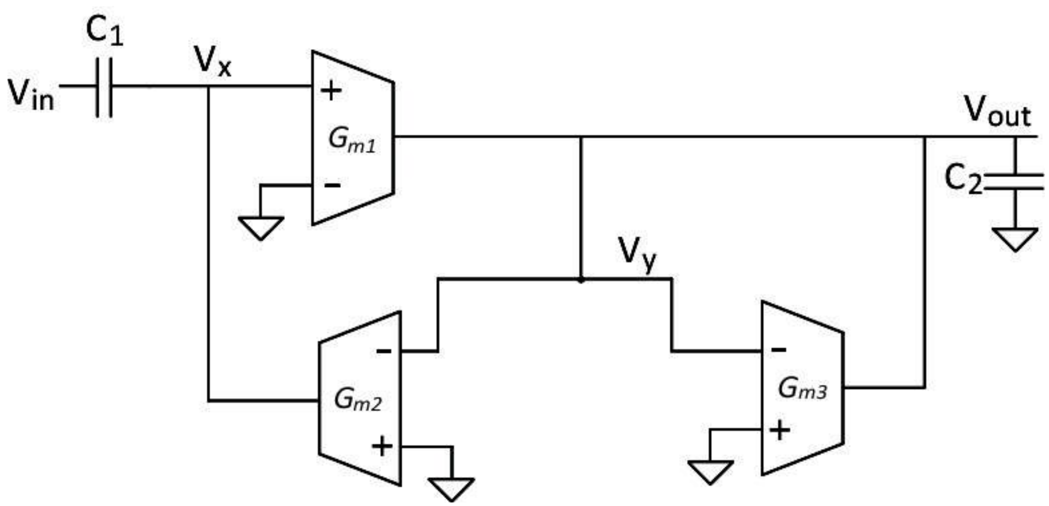

Band-pass Filter Structure

- Gm-C filter with capacitive attenuation, attenuation ratio: A_1=19, A_3=4
- Gain = 1, Q = 4, $|V_x| = |V_y|$
- Fully differential OTA, $G_{m1}=G_{m2}=4G_{m3}$

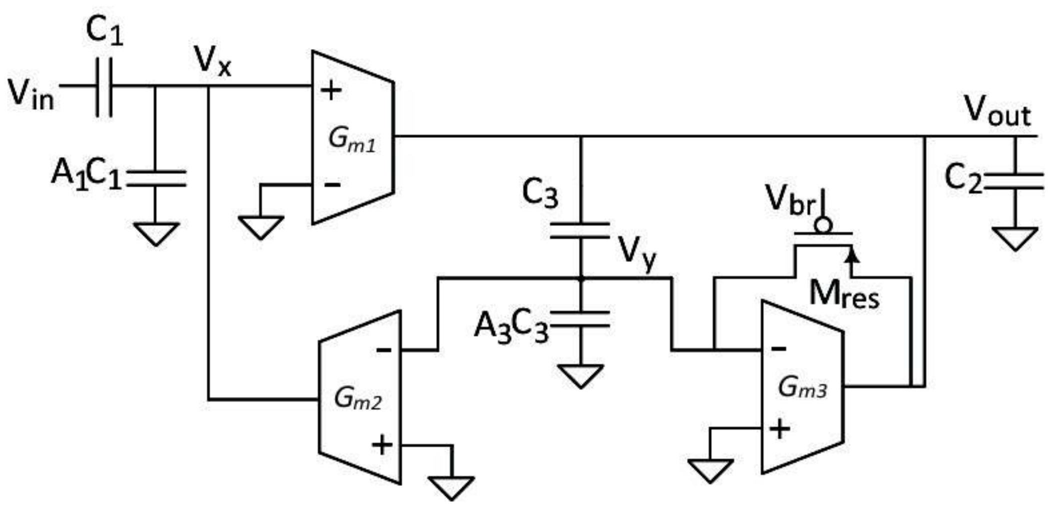

Band-pass Filter Structure

- Gm-C filter with capacitive attenuation, attenuation ratio: A_1=19, A_3=4
- Gain = 1, Q = 4, $|V_x| = |V_y|$
- Fully differential OTA, G_{m1}=G_{m2}=4G_{m3}

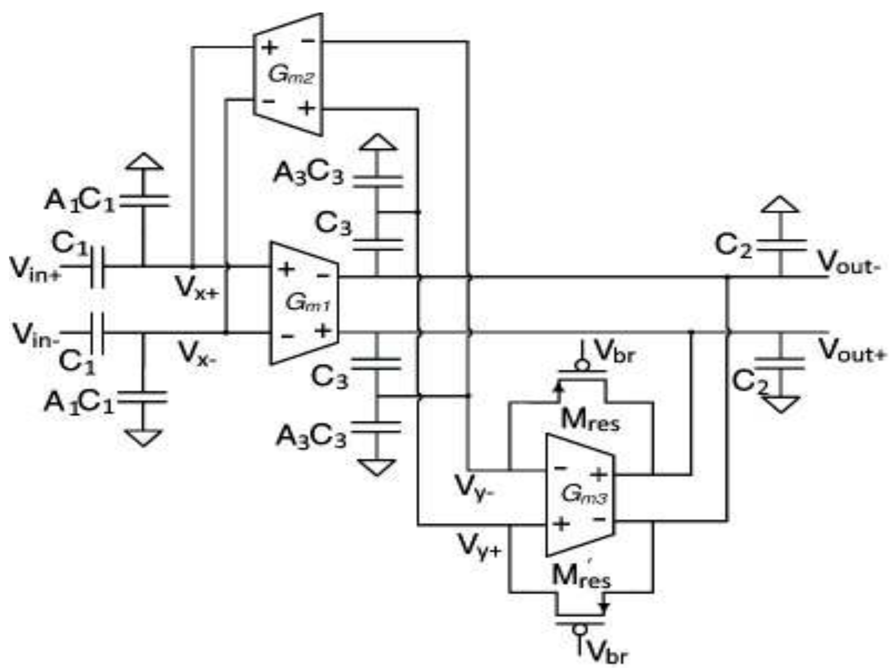

OTA Structure

- **Source degeneration**
- **Current division**
- **M_M is *M* times wider than M_1**
- **Tuning method**
  - fix capacitor value to keep SNR stable
  - M_R overdrive voltage
  - channel length of M_R
  - current division ratio M

triode region, source degeneration resistor

control resistor value

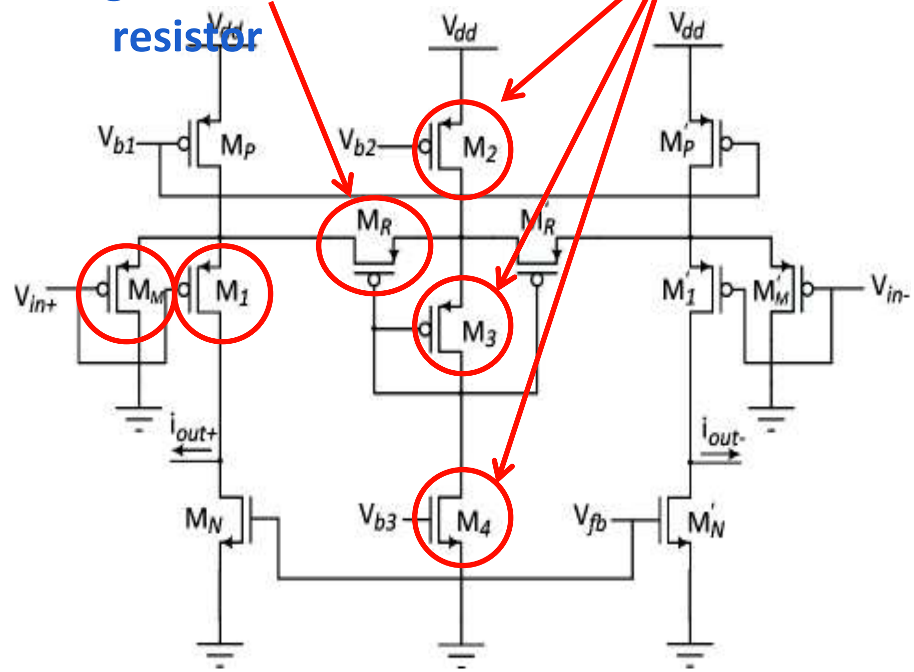

$$G_m = \frac{g_{dsMR}}{\frac{g_{dsMR}}{g_{mM1}} + (M+1)} \approx \frac{g_{dsMR}}{1+M}$$

$$when \quad \frac{g_{dsMR}}{g_{mM1}} << (M+1)$$

Stony Brook University

OTA Simulation

- Simulation environment: Cadence
- MR overdrive voltage: 350mV
- Input peak to peak voltage: 50mV to 300mV
- HD_3=-55dB @ 100mV V_{pp}

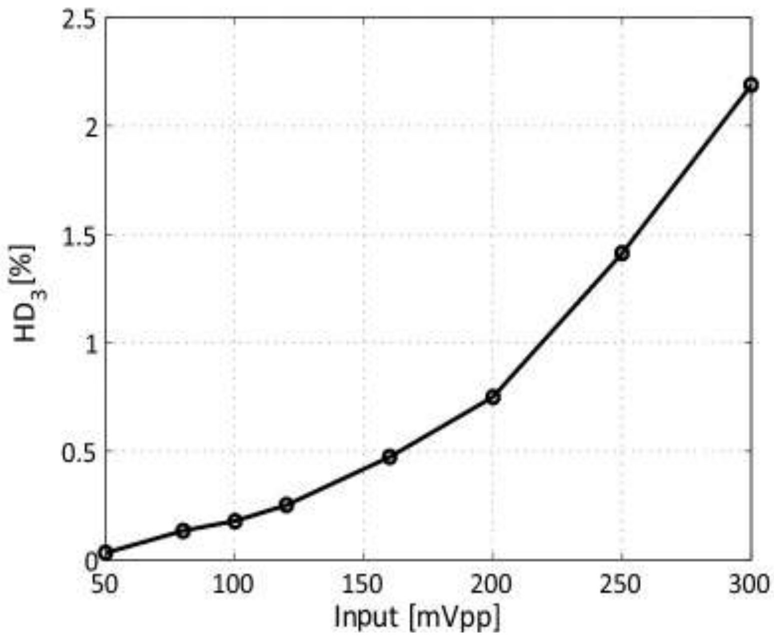

Band-pass Filter Simulation

- Center frequency: 150Hz
- Input signal peak to peak amplitude: 1.92V
- HD3 = -59.6dB
- SNR = 59.9dB

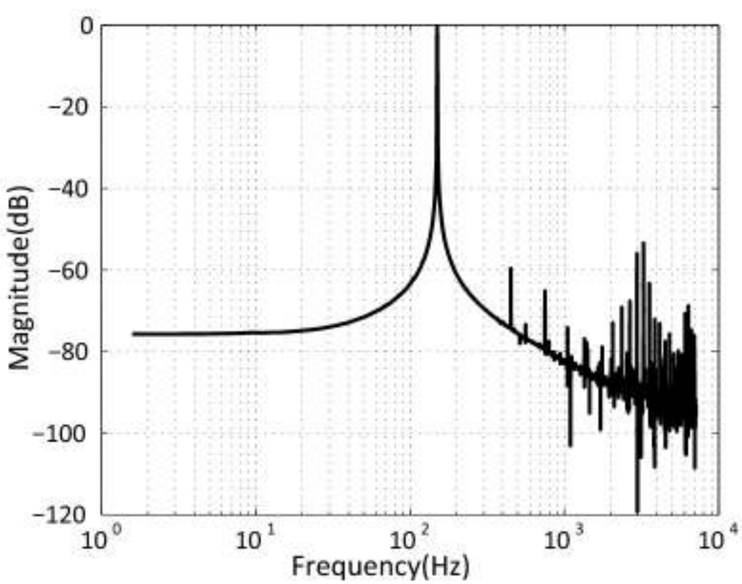

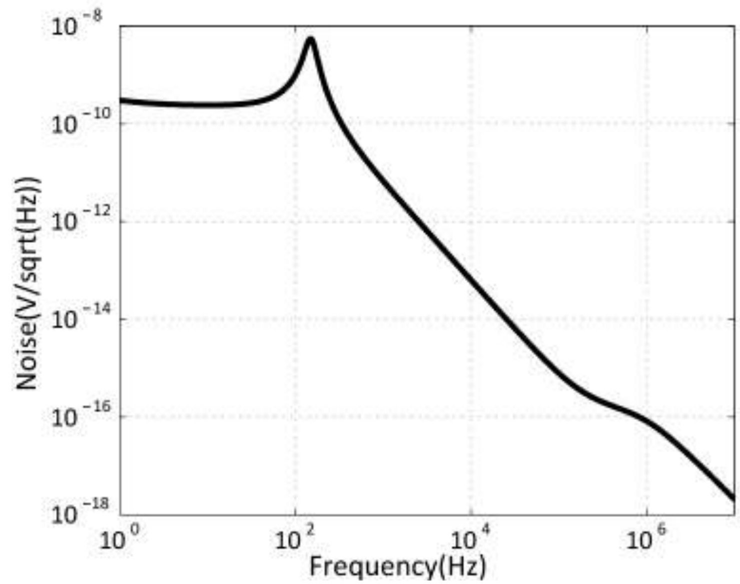

Cochlear Filter Bank

Y. Lin and M. Stanaćević, "A Low-Power, High-Linearity Filter Bank for Auditory Signal Processing Microsystem", *MWSCAS* 2013.

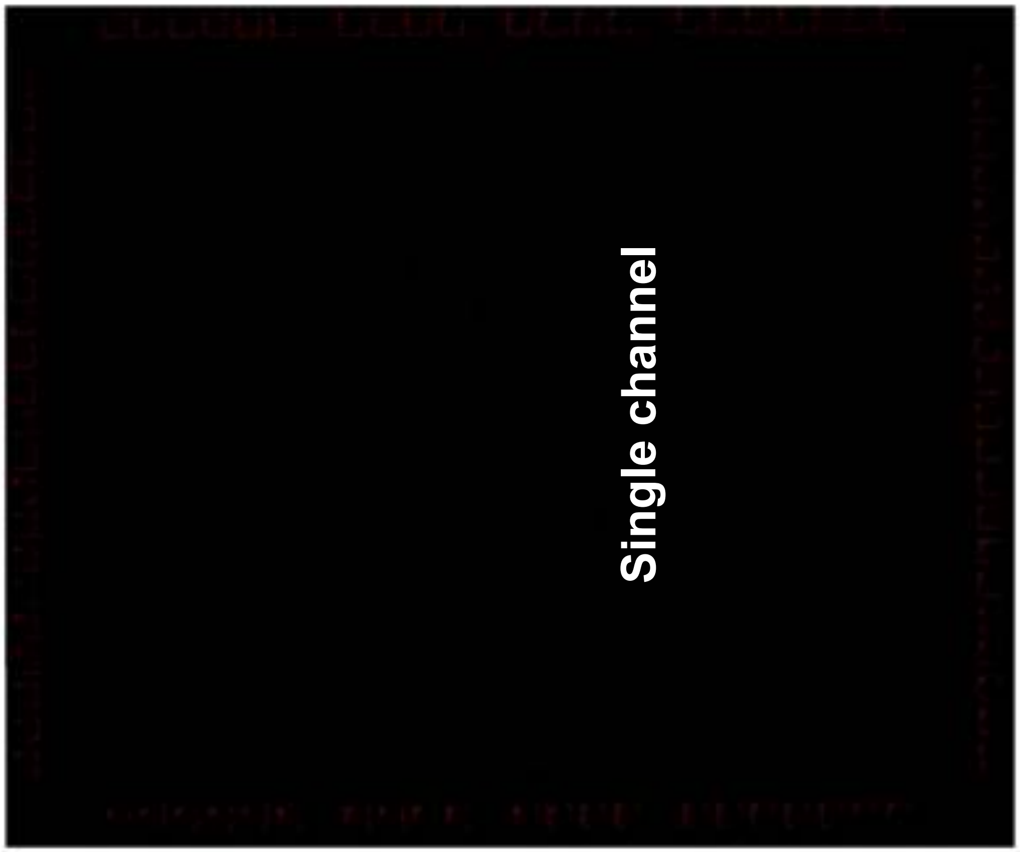

- 0.5μm 3M2P CMOS technology
- 16 channels filter bank and 1 test channel
- Single channel area: 0.16mm^2
- Power consumption: 375 μW

ICA Circuit Architecture

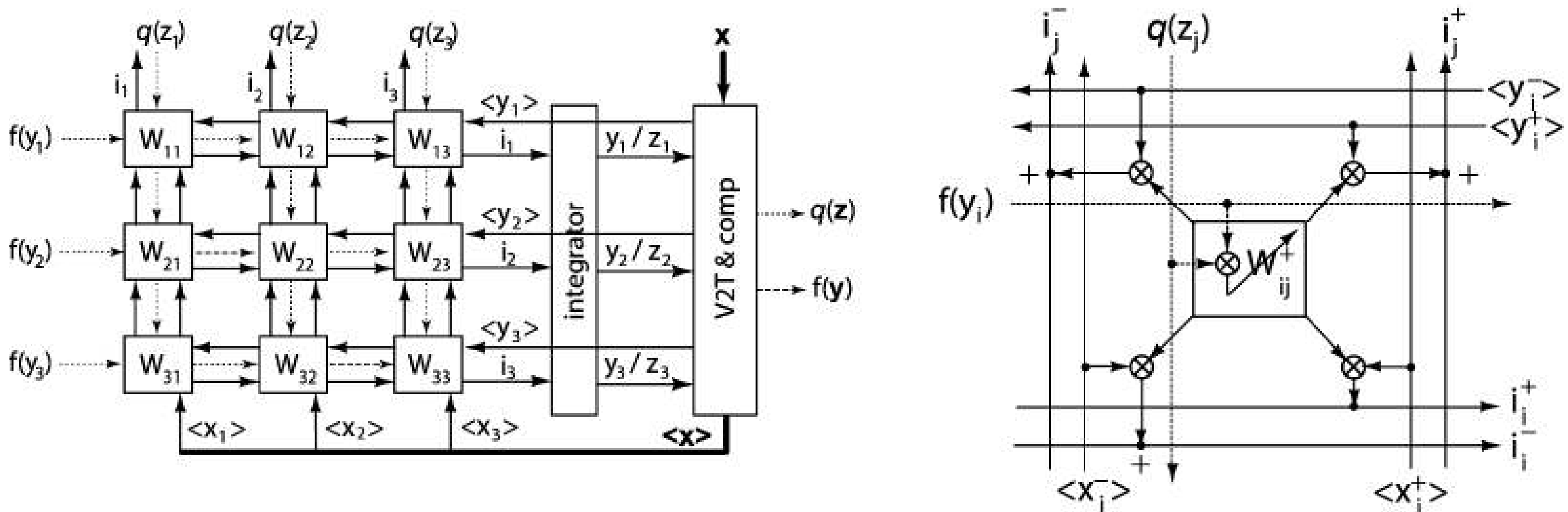

(a) (b)

- **Digitally reconfigurable natural gradient ICA update rule**
  - $\Delta w_{ij} = \mu w_{ij} - \mu f(y_i) z_j$
  - $f(y_i) = \mathrm{sign}(y_i)$, and 3-level quantization of z_j time encoded
- **<xi> and <yi> denote the pulse-width modulated signal of the input signal xi and the output signal yi.**

ICA Update Rule Adaptation

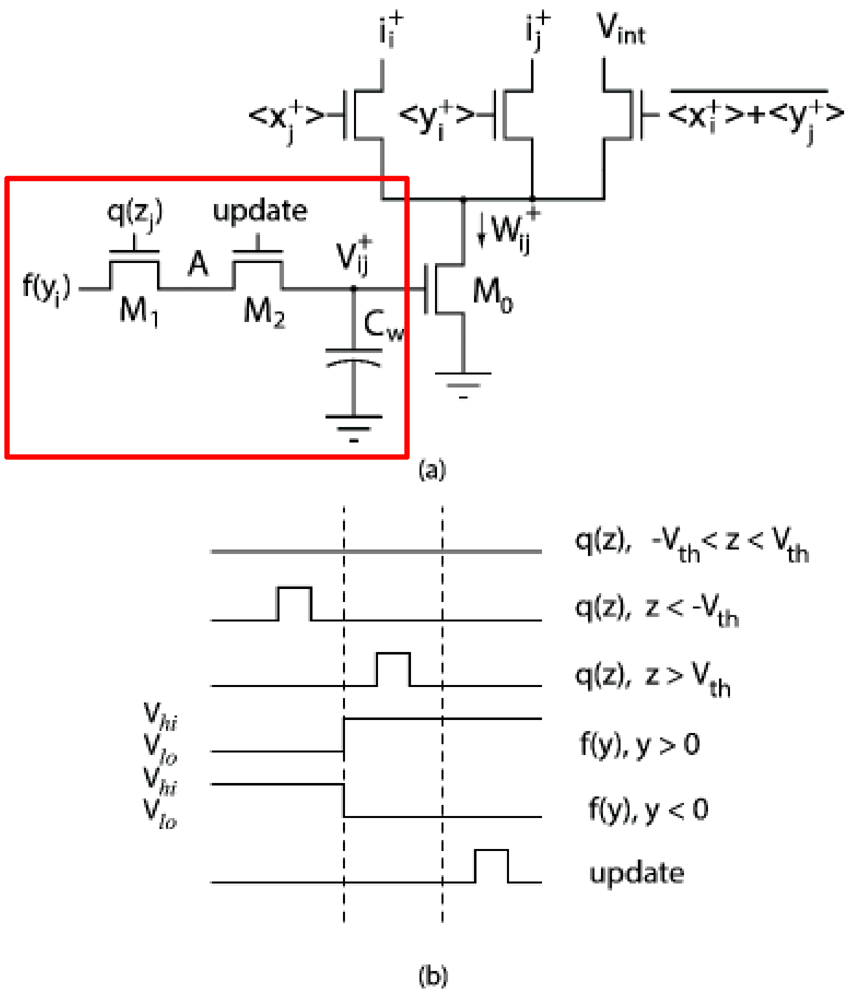

- The 3-level staircase function *q(z)* is approximated with the presence/ absence of the voltage pulse and by the relative position of the pulse.
- The function *f(y)* is coded as a two-level signal, with the *sign(y)* determining the order of the levels V_{lo} and V_{hi}.
- The resulting change on the capacitor is given by

$$V_{ij}^{+}[n+1] = V_{ij}^{+}[n] + \frac{C_p}{C_w + C_p}\left(V_{Aij}^{+}[n] - V_{ij}^{+}[n]\right)$$

Vector-Matrix Multiplication

$$\mathbf{y} = W\mathbf{x} \qquad \mathbf{z} = W^T\mathbf{y}$$

- The vector-matrix multiplications are implemented by integrating switched currents controlled by a PWM signal.

- To minimize the chip area, the two multiplications and the quantization of the signal z are implemented in three phases using the same the integration and voltage-to-time conversion circuitry.

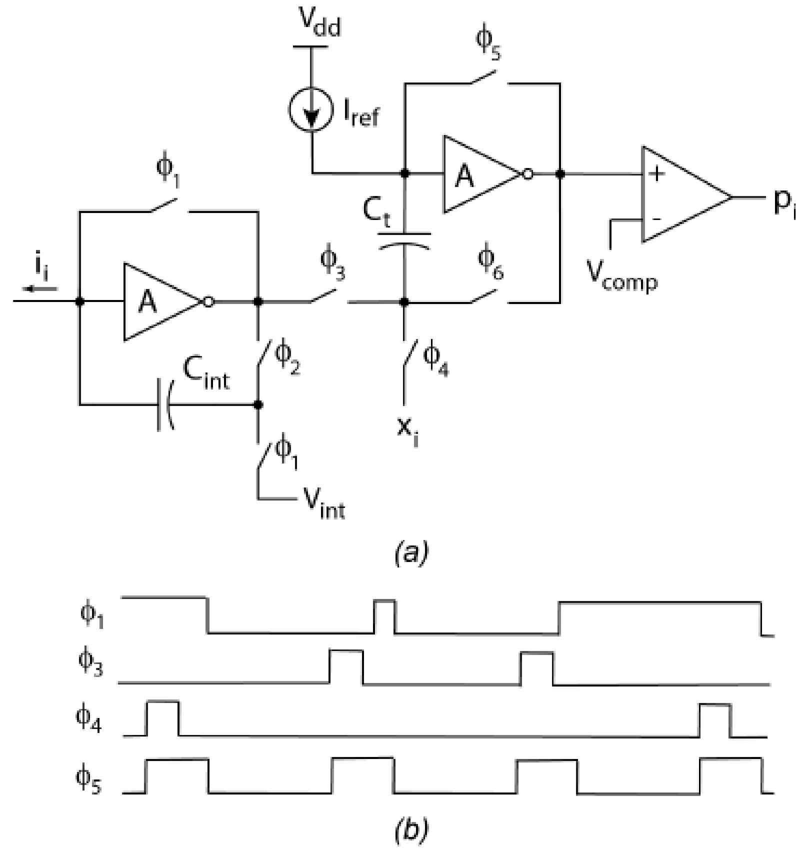

(a)

(b)

- A comparison of the decreasing voltage ramp at the output node of the amplifier with a reference voltage *Vcomp* generates a pulsed signal with a width proportional to the input.

Quantization

- As the pulse-width modulated output signals < yi+ > and < yi- > are available, with a single D-latch the sign of the yi is determined.
- To generate the quantized signal q(zj), a comparison with a positive and a negative threshold voltage Vth is required.

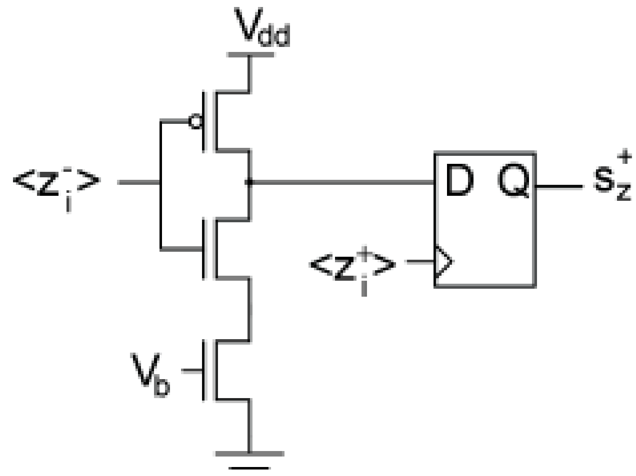

- The comparison with the threshold voltage is performed by delaying one of these pulses before the connection to the input of the D-latch.
- Voltage Vb controls the threshold voltage by controlling the delay time.

Simulation Results

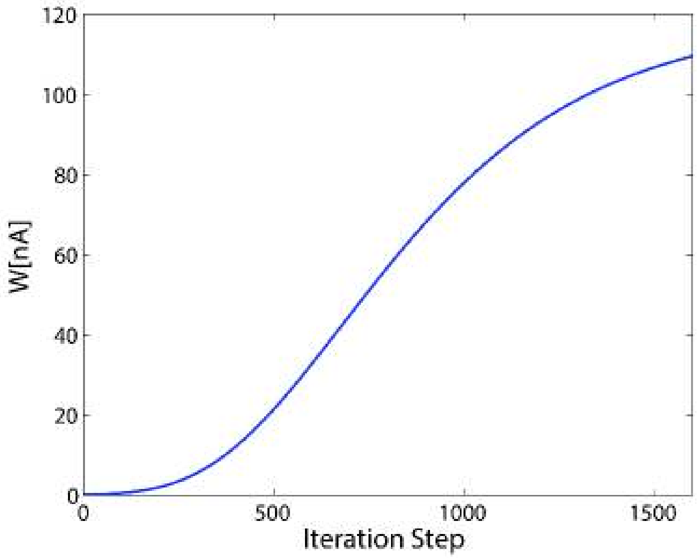

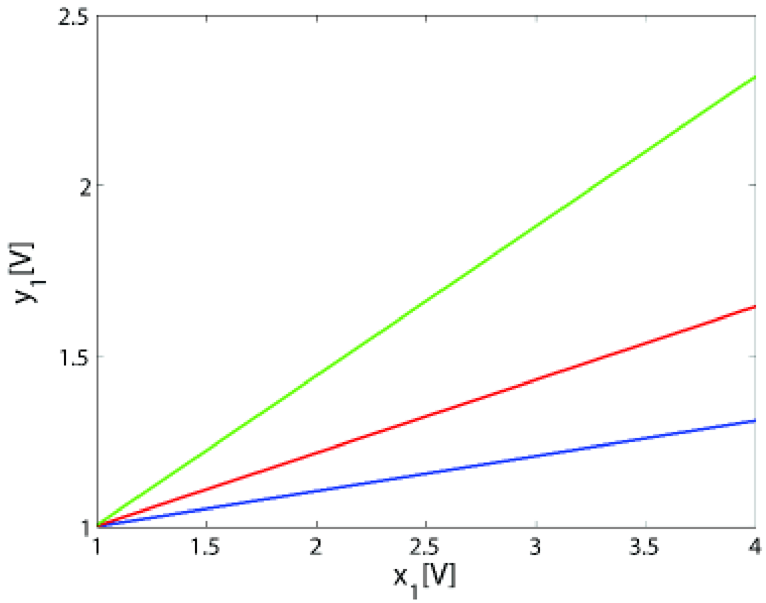

- The adaptation cell is simulated with a constant sign of update.
- The incremental values of the unmixing coefficient as the current of transistor M_0 are shown.

- The output voltage of the integrator y_1 is shown for three different values of the unmixing coefficient w_{11} while the other current sources representing unmixing coefficients are switched off.
- Measured linearity of matrix-vector multiplication is 0.05%.

ICA VLSI Processor

S. Li and M. Stanaćević, "Mixed-signal VLSI Independent Component Analyzer for Hearing Aid Applications", EMBC 2014.

- Technology 0.5 μm 2P3M CMOS
- Area: 0.49 mm^2
- Supply: 5V
- Power dissipation: 80μW
- Separation: 8dB – 13dB

Conclusions

- Wave gradient “flow” converts the problem to that of static ICA, with unmixing coefficients yielding the direction cosines of the sources.
- The technique works for arrays of dimensions smaller than the shortest wavelength in the sources.
- Localization and separation performance is independent of aperture, provided that differential sensitivity be large enough so that ambient interference noise dominates acquisition error noise.
- High resolution delay estimation for source localization using miniature sensor arrays and blind separation of mixed signals with reconfigurable adaptation, have been experimentally demonstrated.
- System allows integration with sensor array for small, compact, battery-operated “smart” sensor applications in surveillance and hearing aids.

Acknowledgment

- IML students Shuo Li (now with Second Sight), Yingkan Lin (now with OmniVision) and Xiao Yun (now with Synopsys).
- This work was supported by the National Science Foundation CAREER Award 0846265.
- The chips were fabricated through the MOSIS foundry service.